

# ENGINEERING OF BIOMATERIALS

INŻYNIERIA BIOMATERIAŁÓW

JOURNAL OF POLISH SOCIETY FOR BIOMATERIALS AND FACULTY OF MATERIALS SCIENCE AND CERAMICS AGH-UST

CZASOPISMO POLSKIEGO STOWARZYSZENIA BIOMATERIAŁÓW I WYDZIAŁU INŻYNIERII MATERIAŁOWEJ I CERAMIKI AGH

**Number 168**

Numer 168

**Volume XXVI**

Rocznik XXVI

**Year 2023**

(Issue 1)

Rok 2023

(Zeszyt 1)

**ISSN 1429-7248**

**PUBLISHER:**

WYDAWCA:

**Polish Society  
for Biomaterials  
in Krakow**

Polskie  
Stowarzyszenie  
Biomateriałów  
w Krakowie

**EDITORIAL  
COMMITTEE:**

KOMITET  
REDAKCYJNY:

**Editor-in-Chief**

Redaktor naczelny

**Elżbieta Pamuła**

**Editor**

Redaktor

**Patrycja**

**Domalik-Pyzik**

**Secretary of editorial**

Sekretarz redakcji

**Design**

Projekt

**Katarzyna Trała**

**ADDRESS OF  
EDITORIAL OFFICE:**

ADRES REDAKCJI:

**AGH-UST**

**30/A3, Mickiewicz Av.**

**30-059 Krakow, Poland**

Akademia

Górniczno-Hutnicza

al. Mickiewicza 30/A-3

30-059 Kraków

**Issue: 250 copies**

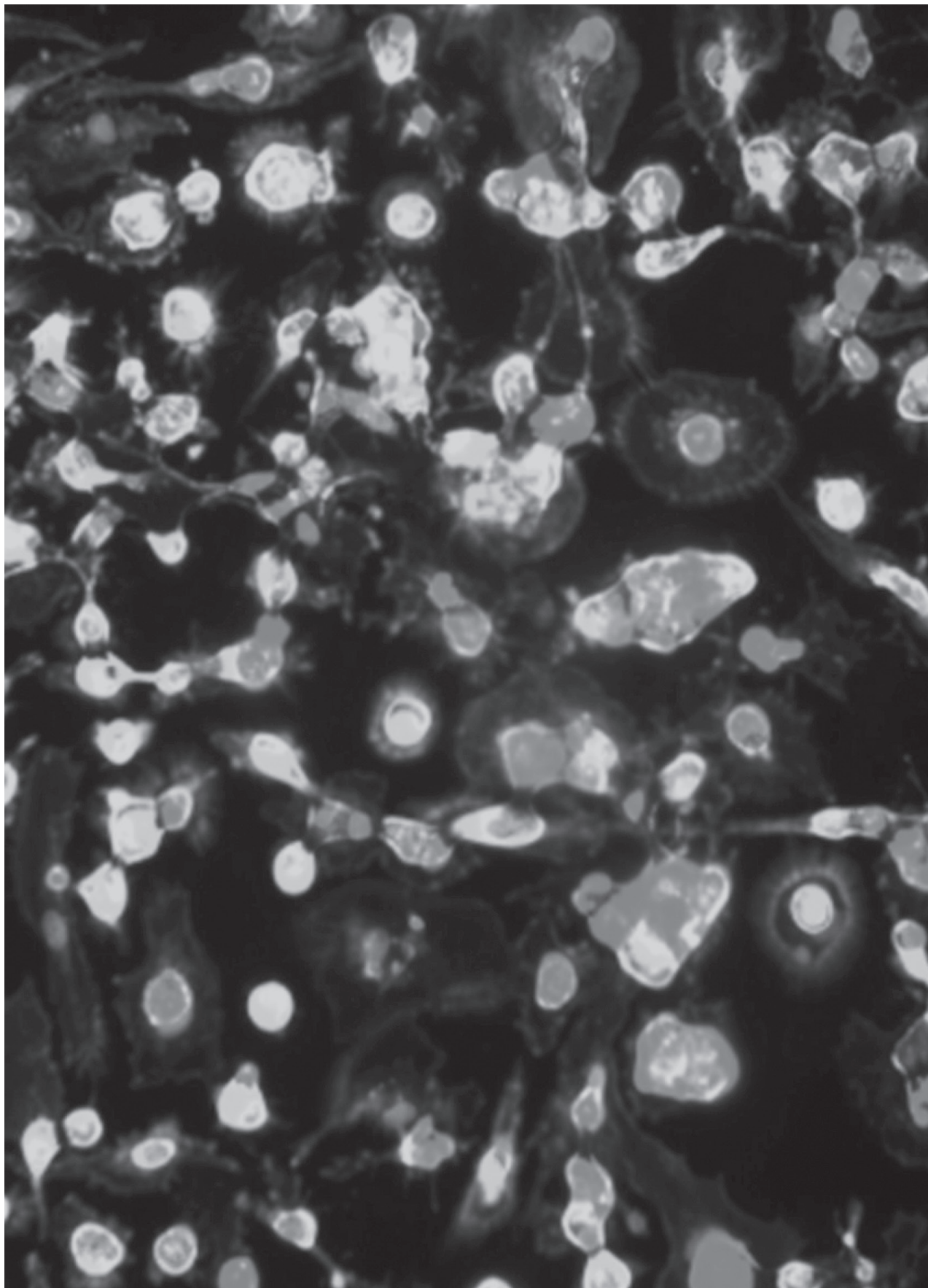
Nakład: 250 egz.

**Scientific Publishing  
House AKAPIT**

Wydawnictwo Naukowe

AKAPIT

e-mail: [wn@akapit.krakow.pl](mailto:wn@akapit.krakow.pl)



**EDITORIAL BOARD  
KOMITET REDAKCYJNY**

**EDITOR-IN-CHIEF**

Elżbieta Pamuła - AGH UNIVERSITY OF SCIENCE AND TECHNOLOGY, KRAKOW, POLAND

**EDITOR**

Patrycja Domalik-Pyzik - AGH UNIVERSITY OF SCIENCE AND TECHNOLOGY, KRAKOW, POLAND

**INTERNATIONAL EDITORIAL BOARD  
MIĘDZYNARODOWY KOMITET REDAKCYJNY**

Iulian Antoniac - UNIVERSITY POLITEHNICA OF BUCHAREST, ROMANIA

Lucie Bacakova - ACADEMY OF SCIENCE OF THE CZECH REPUBLIC, PRAGUE, CZECH REPUBLIC

Romułd Będziński - UNIVERSITY OF ZIELONA GÓRA, POLAND

Marta Błażewicz - AGH UNIVERSITY OF SCIENCE AND TECHNOLOGY, KRAKOW, POLAND

Stanisław Błażewicz - AGH UNIVERSITY OF SCIENCE AND TECHNOLOGY, KRAKOW, POLAND

Wojciech Chrzanowski - UNIVERSITY OF SYDNEY, AUSTRALIA

Jan Ryszard Dąbrowski - BIAŁYSTOK TECHNICAL UNIVERSITY, POLAND

Timothy Douglas - LANCASTER UNIVERSITY, UNITED KINGDOM

Christine Dupont - UNIVERSITÉ CATHOLIQUE DE LOUVAIN, BELGIUM

Matthias Epple - UNIVERSITY OF DUISBURG-ESSEN, GERMANY

Robert Hurt - BROWN UNIVERSITY, PROVIDENCE, USA

James Kirkpatrick - JOHANNES GUTENBERG UNIVERSITY, MAINZ, GERMANY

Ireneusz Kotela - CENTRAL CLINICAL HOSPITAL OF THE MINISTRY OF THE INTERIOR AND ADMINISTR. IN WARSAW, POLAND

Małgorzata Lewandowska-Szumieł - MEDICAL UNIVERSITY OF WARSAW, POLAND

Jan Marciniak - SILESIA UNIVERSITY OF TECHNOLOGY, ZABRZE, POLAND

Ion N. Mihailescu - NATIONAL INSTITUTE FOR LASER, PLASMA AND RADIATION PHYSICS, BUCHAREST, ROMANIA

Sergey Mikhalovsky - UNIVERSITY OF BRIGHTON, UNITED KINGDOM

Stanisław Mitura - TECHNICAL UNIVERSITY OF LIBEREC, CZECH REPUBLIC

Piotr Niedzielski - TECHNICAL UNIVERSITY OF LODZ, POLAND

Abhay Pandit - NATIONAL UNIVERSITY OF IRELAND, GALWAY, IRELAND

Stanisław Pielka - WROCLAW MEDICAL UNIVERSITY, POLAND

Vehid Salih - UCL EASTMAN DENTAL INSTITUTE, LONDON, UNITED KINGDOM

Jacek Składzień - JAGIELLONIAN UNIVERSITY, COLLEGIUM MEDICUM, KRAKOW, POLAND

Andrei V. Stanishevsky - UNIVERSITY OF ALABAMA AT BIRMINGHAM, USA

Anna Ślósarczyk - AGH UNIVERSITY OF SCIENCE AND TECHNOLOGY, KRAKOW, POLAND

Tadeusz Trzaska - UNIVERSITY SCHOOL OF PHYSICAL EDUCATION, POZNAŃ, POLAND

Dimitris Tsipas - ARISTOTLE UNIVERSITY OF THESSALONIKI, GREECE

## Wskazówki dla autorów

1. Prace do opublikowania w kwartalniku „Engineering of Biomaterials / Inżynieria Biomateriałów” przyjmowane będą wyłącznie w języku angielskim.

2. Wszystkie nadsyłane artykuły są recenzowane.

3. Materiały do druku prosimy przysyłać za pomocą systemu online ([www.biomaterials.pl](http://www.biomaterials.pl)).

4. Struktura artykułu:

• TYTUŁ • Autorzy i instytucje • Streszczenie (200-250 słów) • Słowa kluczowe (4-6) • Wprowadzenie • Materiały i metody • Wyniki i dyskusja • Wnioski • Podziękowania • Piśmiennictwo

5. Autorzy przesyłają pełną wersję artykułu, łącznie z ilustracjami, tabelami, podpisami i literaturą w jednym pliku. Artykuł w tej formie przesyłany jest do recenzentów. Dodatkowo autorzy proszeni są o przesłanie materiałów ilustracyjnych (rysunki, schematy, fotografie, wykresy) w oddzielnych plikach (format np. .jpg, .gif, .tiff, .bmp). Rozdzielczość rysunków min. 300 dpi. Wszystkie rysunki i wykresy powinny być czarno-białe lub w odcieniach szarości i ponumerowane cyframi arabskimi. W tekście należy umieścić odnośniki do rysunków i tabel.

6. Na końcu artykułu należy podać wykaz piśmiennictwa w kolejności cytowania w tekście i kolejno ponumerowany.

7. Redakcja zastrzega sobie prawo wprowadzenia do opracowań autorskich zmian terminologicznych, poprawek redakcyjnych, stylistycznych, w celu dostosowania artykułu do norm przyjętych w naszym czasopiśmie. Zmiany i uzupełnienia merytoryczne będą dokonywane w uzgodnieniu z autorem.

8. Opinia lub uwagi recenzentów będą przekazywane Autorowi do ustosunkowania się. Nie dostarczenie poprawionego artykułu w terminie oznacza rezygnację Autora z publikacji pracy w naszym czasopiśmie.

9. Za publikację artykułów redakcja nie płaci honorarium autorskiego.

10. Adres redakcji:

Czasopismo

„Engineering of Biomaterials / Inżynieria Biomateriałów”

Akademia Górniczo-Hutnicza im. St. Staszica

Wydział Inżynierii Materiałowej i Ceramiki

al. Mickiewicza 30/A-3, 30-059 Kraków

tel. (48) 12 617 44 48, 12 617 25 61

e-mail: [epamula@agh.edu.pl](mailto:epamula@agh.edu.pl), [kabe@agh.edu.pl](mailto:kabe@agh.edu.pl)

Szczegółowe informacje dotyczące przygotowania manuskryptu oraz procedury recenzowania dostępne są na stronie internetowej czasopisma:

[www.biomaterials.pl](http://www.biomaterials.pl)

## Instructions for authors

1. Papers for publication in quarterly journal „Engineering of Biomaterials / Inżynieria Biomateriałów” should be written in English.

2. All articles are reviewed.

3. Manuscripts should be submitted to editorial office through online submission system ([www.biomaterials.pl](http://www.biomaterials.pl)).

4. A manuscript should be organized in the following order:

• TITLE • Authors and affiliations • Abstract (200-250 words) • Keywords (4-6) • Introduction • Materials and Methods • Results and Discussion • Conclusions • Acknowledgements • References

5. All illustrations, figures, tables, graphs etc. preferably in black and white or grey scale should be additionally sent as separate electronic files (format .jpg, .gif, .tiff, .bmp). High-resolution figures are required for publication, at least 300 dpi. All figures must be numbered in the order in which they appear in the paper and captioned below. They should be referenced in the text. The captions of all figures should be submitted on a separate sheet.

6. References should be listed at the end of the article. Number the references consecutively in the order in which they are first mentioned in the text.

7. The Editors reserve the right to improve manuscripts on grammar and style and to modify the manuscripts to fit in with the style of the journal. If extensive alterations are required, the manuscript will be returned to the authors for revision.

8. Opinion or notes of reviewers will be transferred to the author. If the corrected article will not be supplied on time, it means that the author has resigned from publication of work in our journal.

9. Editorial does not pay author honorarium for publication of article.

10. Address of editorial office:

Journal

„Engineering of Biomaterials / Inżynieria Biomateriałów”

AGH University of Science and Technology

Faculty of Materials Science and Ceramics

30/A-3, Mickiewicz Av., 30-059 Krakow, Poland

tel. (48) 12) 617 44 48, 12 617 25 61

e-mail: [epamula@agh.edu.pl](mailto:epamula@agh.edu.pl), [kabe@agh.edu.pl](mailto:kabe@agh.edu.pl)

Detailed information concerning manuscript preparation and review process are available at the journal's website:

[www.biomaterials.pl](http://www.biomaterials.pl)





# 32<sup>nd</sup> Biomaterials in Medicine and Veterinary Medicine Annual Conference

12 – 15 October 2023 Rytro, Poland

SAVE THE DATE

12-15

OCTOBER  
2023

[www.biomat.agh.edu.pl](http://www.biomat.agh.edu.pl)



REGISTER  
AND  
SUBMIT  
AN ABSTRACT



## **SPIS TREŚCI CONTENTS**

- MANUFACTURING AND CHARACTERIZATION  
OF GELLAN GUM – ZINC OXIDE COMPOSITES  
AS POTENTIAL BIOMATERIALS  
FOR WOUND TREATMENT**  
ALICJA MACYK, ANNA KUSIBAB,  
ELŻBIETA PAMUŁA **2**
- THE PROPERTIES OF FISH COLLAGEN  
FILMS AFTER CROSS-LINKING  
WITH TANNIC ACID**  
ALINA SIONKOWSKA, KATARZYNA LEWANDOWSKA,  
MARTA SZULC, PATRYCJA BRUDZYŃSKA,  
KAROLINA KULKA, ŁUKASZ PIWOWARSKI **9**
- CURCUMIN DELIVERY SYSTEMS AS  
DRESSING COMPONENTS FOR THE  
TREATMENT OF DIABETIC FOOT ULCERS:  
TESTS ON MACROPHAGES POLARIZATION**  
KAROLINA WÓJCIK, ANNA KUSIBAB,  
ANA BEATRIZ SOUSA, JUDITE NOVAIS  
BARBOSA, ELŻBIETA PAMUŁA **15**
- CHARACTERISTIC OF FISH COLLAGEN  
FILMS CROSS-LINKED WITH  
GLUTARALDEHYDE**  
KAROLINA KULKA-KAMIŃSKA,  
PATRYCJA BRUDZYŃSKA, ALINA SIONKOWSKA,  
KATARZYNA LEWANDOWSKA,  
ŁUKASZ PIWOWARSKI **25**

# MANUFACTURING AND CHARACTERIZATION OF GELLAN GUM – ZINC OXIDE COMPOSITES AS POTENTIAL BIOMATERIALS FOR WOUND TREATMENT

ALICJA MACYK <sup>\*</sup>, ANNA KUSIBAB ,  
ELŻBIETA PAMUŁA 

AGH UNIVERSITY OF KRAKOW,  
FACULTY OF MATERIALS SCIENCE AND CERAMICS,  
DEPARTMENT OF BIOMATERIALS AND COMPOSITES,  
AL. A. MICKIEWICZA 30, 30-059 KRAKOW, POLAND  
<sup>\*</sup>E-MAIL: AMACYK@STUDENT.AGH.EDU.PL

## Abstract

*This study aimed to produce gellan gum-based hydrogels with the addition of zinc oxide as a potential dressing material. Hydrogels with ZnO concentrations of 0.01%, 0.02% and 0.04% were prepared, micrometric and nanometric ZnO particles were used, and a CaCl<sub>2</sub> crosslinker was added to one part of the samples. All samples (14 types) produced by the freeze drying method were characterized with high swelling properties (>2000%), what is important to ensure the absorption of exudates from wounds. Samples with ZnO particles cross-linked with CaCl<sub>2</sub> lost less mass after incubation in aqueous media and were characterized by better dimensional stability than those without crosslinking. The pH of the extracts of the samples containing ZnO particles was more neutral (pH 7.0-7.6) than that of the control gellan gum samples (pH of 5.5-6.1). The zinc release from cross-linked samples was twice as high for those containing nanometric particles than for micrometric particles (1.94 ± 0.04 mg/l and 0.93 ± 0.02, respectively). Relatively large amounts of released zinc species in the case of samples containing ZnO nanoparticles are promising in the context of the antibacterial properties and treatment of infected wounds. A lower amount of zinc released from samples with ZnO microparticles could be sufficient to prevent the development of the infection. Furthermore, both materials show satisfactory cytocompatibility with L929 fibroblasts, as shown by Alamar blue and live/dead viability tests, making them prospective candidates for wound healing.*

**Keywords:** gellan gum, zinc oxide nanoparticles, zinc oxide microparticles, wound healing, L929 fibroblasts

## Introduction

Hydrogels are materials widely used as wound dressings. Due to their high water content, they provide a moist environment that promotes wound healing and also allows gas exchange. Hydrogels adhere very well to the wound, thus preventing contamination of damaged tissue, and at the same time, they do not stick to it, so changing the hydrogel dressing is painless [1]. In addition, especially when hydrogels are processed by freeze-drying to form porous sponges, they can absorb exudate from the wound and cleanse it of necrotic tissues [2]. Hydrogels are usually formed by synthetic polymers, e.g., poly(vinyl alcohol) (PVA), poly(vinyl pyrrolidone) (PVP) and poly(ethylene glycol) (PEG) or by natural polysaccharides such as starch, cellulose, chitosan, agar, alginates or gellan gum [3].

Gellan gum is a biodegradable and nontoxic polysaccharide, obtained in the fermentation process by *Sphingomonas elodea* bacteria [4]. It is used in the food industry because of its gelling properties and as a stabiliser of suspensions; it is also applied in the medical industry, for example, in tissue engineering as a matrix of scaffolds or as a drug carrier [5,6]. Gellan gum hydrogels are most often cross-linked using calcium ions [7]. Gellan gum-based materials supplemented with lipid nanoparticles loaded with antibacterial peptide, nisin, have already been developed as potential dressing materials for infected wounds [8].

Zinc oxide is known for its antibacterial properties that may have a beneficial effect on wound healing [9]. The antibacterial effect of ZnO is related to the production of reactive oxygen species (ROS) that destroy the bacterial cell wall. It can also release zinc ions, Zn<sup>2+</sup>, which are absorbed by the bacterial cell, damaging DNA, and reacting with intracellular proteins [10]. ZnO is also a potential cross-linker, improving the mechanical properties of polysaccharide hydrogels, as well as increasing resistance to degradation [11].

The purpose of this study was to develop dressing materials based on gellan gum supplemented with zinc oxide particles. To this end, several sample types were manufactured that differed in ZnO particle size (nanometric or micrometric) and particle concentration. Then, physico-chemical properties of the samples including dimensional stability, swelling properties, and zinc release were assessed. The study also aimed at checking the cross-linking properties of ZnO powders depending on the concentration and particle size and its effect on the properties of the resulting materials. In addition, cytotoxicity tests with the use of L929 fibroblasts of all studied materials were performed to find out which has the most promising properties for application as wound dressings.

## Materials and Methods

### Preparation of gellan gum samples with zinc oxide particles

Gellan gum (GG, low-acyl, Sigma Aldrich, USA), nanometric ZnO (<100 nm particle size, Sigma-Aldrich, USA) and micrometric ZnO (<50 µm particle size, ZM Silesia SA, Oława, Poland) were used in this study.

The GG control sample was prepared by dissolving 200 mg of GG in 10 ml of UHQ ultrapure water for 30 min in a 90°C water bath. The suspension was vortexed for 10 s and poured into a glass Petri dish (diameter 9 cm). Spacers placed in a Petri dish made it possible to obtain a uniform hydrogel height of 4 mm.

[*Engineering of Biomaterials* 168 (2023) 2-8]

doi:10.34821/eng.biomat.168.2023.2-8

Submitted: 2023-03-28, Accepted: 2023-04-26, Published: 2023-05-08



Copyright © 2023 by the authors. Some rights reserved.  
Except otherwise noted, this work is licensed under  
<https://creativecommons.org/licenses/by/4.0>

The cross-linked GG control sample (GG+CaCl<sub>2</sub>) was prepared by dissolving 222 mg of GG in 10 ml of ultrapure UHQ water for 30 min in a 90°C water bath. The temperature was then reduced to 70°C and the crosslinking solution (1% CaCl<sub>2</sub> solution) was heated in a water bath: 493 mg CaCl<sub>2</sub>·6H<sub>2</sub>O in 24.76 ml UHQ water. Then 9 ml of the GG suspension and 1 ml of the crosslinking solution were taken, vortexed for 10 s and poured into a Petri dish (diameter 9 cm) with spacers. The final concentration of CaCl<sub>2</sub> in the samples was 0.1%.

The GG samples with the addition of ZnO at concentrations of 0.01 wt%, 0.02 wt%, and 0.04 wt% were also prepared by weighing the appropriate amount of ZnO (1.1 mg, 2.2 mg, 4.4 mg, respectively), which was suspended in 11 ml of UHQ water using ultrasound for 30 min. 220 mg of GG were weighed and mixed with ZnO suspension, then heated for 30 min in a water bath at 90°C. 10 ml of suspension was taken, vortexed for 10 s, and poured into a Petri dish (diameter 9 cm) with spacers. Two ZnO powder grades were used: nanometric (n) and micrometric (m), resulting in six sample types: GG+ZnO(n)0.01%, GG+ZnO(n)0.02%, GG+ZnO(n)0.04%, GG+ZnO(m)0.01%, GG+ZnO(m)0.02%+CaCl<sub>2</sub>, GG+ZnO(m)0.04%.

The GG+CaCl<sub>2</sub> samples with the addition of ZnO at concentrations of 0.01 wt%, 0.02 wt%, and 0.04 wt% were also prepared by weighing the appropriate amount of ZnO (1.1 mg, 2.2 mg, 4.4 mg, respectively), which was suspended in 11 ml of UHQ water using ultrasound for 30 min. 220 mg of GG were weighed and mixed with ZnO suspension, then heated for 30 min in a water bath at 90°C. Then, 9 ml of the suspension and 1 ml of 1% CaCl<sub>2</sub> were taken, vortexed for 10 s, and poured into a Petri dish (diameter of 9 cm) with spacers. Two ZnO powder grades were used: nanometric (n) and micrometric (m), resulting in six sample types: GG+ZnO(n)0.01%+CaCl<sub>2</sub>, GG+ZnO(n)0.02%+CaCl<sub>2</sub>, GG+ZnO(n)0.04%+CaCl<sub>2</sub>, GG+ZnO(m)0.01%+CaCl<sub>2</sub>, GG+ZnO(m)0.02%+CaCl<sub>2</sub>, GG+ZnO(m)0.04%+CaCl<sub>2</sub>.

The hydrogels were cooled at 4°C for 30 min, and then circular samples with a diameter of 12 mm were cut out with a punch device. The hydrogel samples were placed in 24-well plate dishes, frozen at -80°C for 24 h followed by 48 h freeze-drying (Alpha 1-2, Martin Christ, Osterode am Harz, Germany).

### Microscopic observations

The freeze dried samples were observed under a microscope (Keyence VHX 7000, Belgium) at a magnification of 20x. Each of the samples was then immersed in 3 ml of phosphate buffered saline (PBS, Sigma-Aldrich, USA) for 1 h, after which microscopic observations were made again to assess microstructural changes after incubation in PBS.

### Swelling, remaining mass, pH measurements

The freeze dried samples (n = 3 of each type) were weighed on an analytical balance and then immersed in 2 ml of PBS each. After 24 h, the samples were collected, and carefully wiped with a tissue (Kimwipes, KIMTECH) to remove excess water, but avoiding removing water out of the pores of the sample.

The swelling of the samples was calculated from the formula (1):

$$\%Swelling = \frac{M_w - M_d}{M_d} \cdot 100\% \quad (1)$$

where:  $M_w$  - the mass of the wet sample,  $M_d$  - the mass of the dry sample.

After 48 h of incubation in PBS, the samples were washed extensively with UHQ water (4 times, 5 ml of water, 3 min for each wash) and dried at 37°C for 24 h. The dried samples were weighted. The remaining mass of the samples was calculated using the formula (2):

$$\%Remaining\ mass = \frac{M_{deg}}{M_{non-deg}} \cdot 100\% \quad (2)$$

where:  $M_{deg}$  is the mass of the dried sample after 48 h of incubation,  $M_{non-deg}$  is the mass of the dry sample before incubation.

For pH measurements of the incubation medium, previously weighed samples were placed in separate Falcon tubes, and about 3 ml of UHQ water was poured into each tube so that the ratio of sample weight to water volume was constant in each tube and equal to 0.425%. The pH of the samples was measured after 24 h (Elmetron 410 pH Meter, Poland). The pH meter was thoroughly cleaned between measurements. To test the stability of the samples, they were incubated in 3 ml of UHQ water for 7 days. After 7 days, it was checked whether the hydrogels structure changed or degraded.

### Atomic absorption spectrometry

To determine the ZnO release from the hydrogel samples, atomic absorption spectrometry (Perkin-Elmer 3110, USA) was used. Extracts from hydrogel samples after 10 days of incubation in water (the same as those used for the pH measurements) were used for the analysis. The suspensions were centrifuged and 0.5 ml of sample solution of the respective samples was added: GG, GG+CaCl<sub>2</sub>, GG+ZnO(n)0.04%, GG+ZnO(n)0.04%+CaCl<sub>2</sub>, GG+ZnO(m)0.04%, GG+ZnO(m)0.04%+CaCl<sub>2</sub>.

### In vitro cytotoxicity

To test potential cytotoxicity, 1% extracts of the samples were prepared. For this purpose, two samples of each type were weighed. Each sample was irradiated under a UV lamp for 10 min on each side. The samples were placed in Falcons tubes and incubated in cell culture medium (the same as for further *in vitro* tests, 2 ml of medium for 20 mg of samples) for 24 h.

L929 fibroblasts (European Collection of Cell Cultures, UK) were cultured in Dulbecco's modified Eagle's medium (DMEM) supplemented with 10% foetal bovine serum (FBS) and 1% penicillin/streptomycin (all chemicals from PAN-Biotech) at 37°C in a 5% CO<sub>2</sub> atmosphere. A suspension of 50,000 cells/ml of medium was prepared. In a 96-well plate, 200 µL of cell suspension was transferred to each well resulting in 10,000 cells per well and allowed to adhere to the bottom of the plate. After 24 h, the medium was aspirated and replaced with extracts of the samples. Cells were cultured in 1% and 0.5% w/v extracts of the samples as well as in control medium without extracts (n = 3).

Cell viability was tested with the AlamarBlue assay [12]. After 24 h of cell culture with extracts, the medium was aspirated from each well and replaced with 150 µl of a 5% AlamarBlue solution in DMEM. The prepared plate was incubated for 3 h and then 100 µl of medium was transferred to a 96-well black plate. Using the FluoroSTAR Omega reader, the fluorescence intensity of the samples was obtained. The percentage of resazurin reduction was calculated using the formula (3):

$$\%Resazurin\ reduction = \frac{F_x - F_{0\%}}{F_{100\%} - F_{0\%}} \cdot 100\% \quad (3)$$

where:  $F_x$  - fluorescence of the sample,  $F_{0\%}$  - fluorescence of the medium with AlamarBlue reagent without cells,  $F_{100\%}$  - fluorescence of the completely reduced reagent.

For live/dead staining, the extracts were replaced with a solution of 100  $\mu$ l of 0.1% calcein AM (Sigma-Aldrich) and 0.1% propidium iodide (Sigma-Aldrich) solutions in PBS. The plate was incubated for 20 min at 37°C and then a fluorescence microscope (Axiovert 40 CFL, Germany) was used for cell visualization.

### Statistics

Statistical analysis was performed by one-way analysis of variance (one-way ANOVA) using OriginLab2023 software. Differences were considered significant when  $p < 0.05$ . The results are presented as mean  $\pm$  standard deviation (SD).

## Results and Discussion

During hydrogel production, it was observed that with an increase of the ZnO concentration, the samples became stiffer and harder, and the highest stiffness was found for the samples with 0.04% ZnO and CaCl<sub>2</sub> cross-linker. The control sample of neat gellan gum was the softest, so great care had to be taken when cutting the GG hydrogels without damaging the samples.

### Microscopic observations

The results of microscopic observations of dry samples and those after soaking in PBS for 1 h (wet) are shown in FIG. 1. With the increase in the concentration of ZnO, whiter colouration of the samples was observed. Samples with the addition of CaCl<sub>2</sub> cross-linker had larger pores compared to samples without CaCl<sub>2</sub>. The sample of ZnO(n) 0.04%+CaCl<sub>2</sub> had the largest pores. The highest porosity was found for samples containing nanometric ZnO with the addition of a CaCl<sub>2</sub> crosslinker. After soaking in PBS, the size of the samples increased (FIG. 1).

### Swelling, remaining mass, pH measurements

The swelling of the samples after 24 h of incubation in PBS was very high for all samples always exceeding 2000% (TABLE 1, column 2).

The results of the samples' mass measurements after 48 h incubation in PBS (TABLE 1, column 3) show that the addition of ZnO to the non-cross-linked samples caused a higher mass reduction than in the control GG sample. The lowest remaining mass equal to 75% was measured for GG+ZnO(n)0.04% sample. Samples cross-linked with CaCl<sub>2</sub> showed a much higher remaining mass, except GG+ZnO(m)0.01%+CaCl<sub>2</sub> for which the remaining mass was 87%.

The pH measurements (TABLE 1, column 4) show that each sample containing ZnO caused an increase in pH as compared to the GG and GG+CaCl<sub>2</sub> control samples which presumably is due to the release of zinc species from the hydrogels into the solution. The samples with the addition of ZnO showed a pH of 7.0-7.6, while the samples of GG and GG+CaCl<sub>2</sub> had a pH of 5.5 and 6.1, respectively.

The last column of TABLE 1 shows the dimensional stability of the hydrogels. The "yes" mark means that the sample did not degrade within 7 days of incubation in UHQ water, while the mark "no" means that the sample degraded under these conditions.

The results show that all samples crosslinked with CaCl<sub>2</sub>, except GG+ZnO(m)0.01%+CaCl<sub>2</sub>, were dimensionally stable up to 7 days immersion in UHQ water. The latter sample was also characterized by a higher loss of mass of 13% and a very high swelling that reached 3700  $\pm$  300%. On the other hand, the only one sample without CaCl<sub>2</sub>, i.e. GG+ZnO(m)0.04%, was dimensionally stable after 7 days of incubation. It had a relatively low swelling of 2250  $\pm$  300% and lost only 8% of its mass after incubation. The other samples without CaCl<sub>2</sub> crosslinking dissolved within 7 days of incubation.

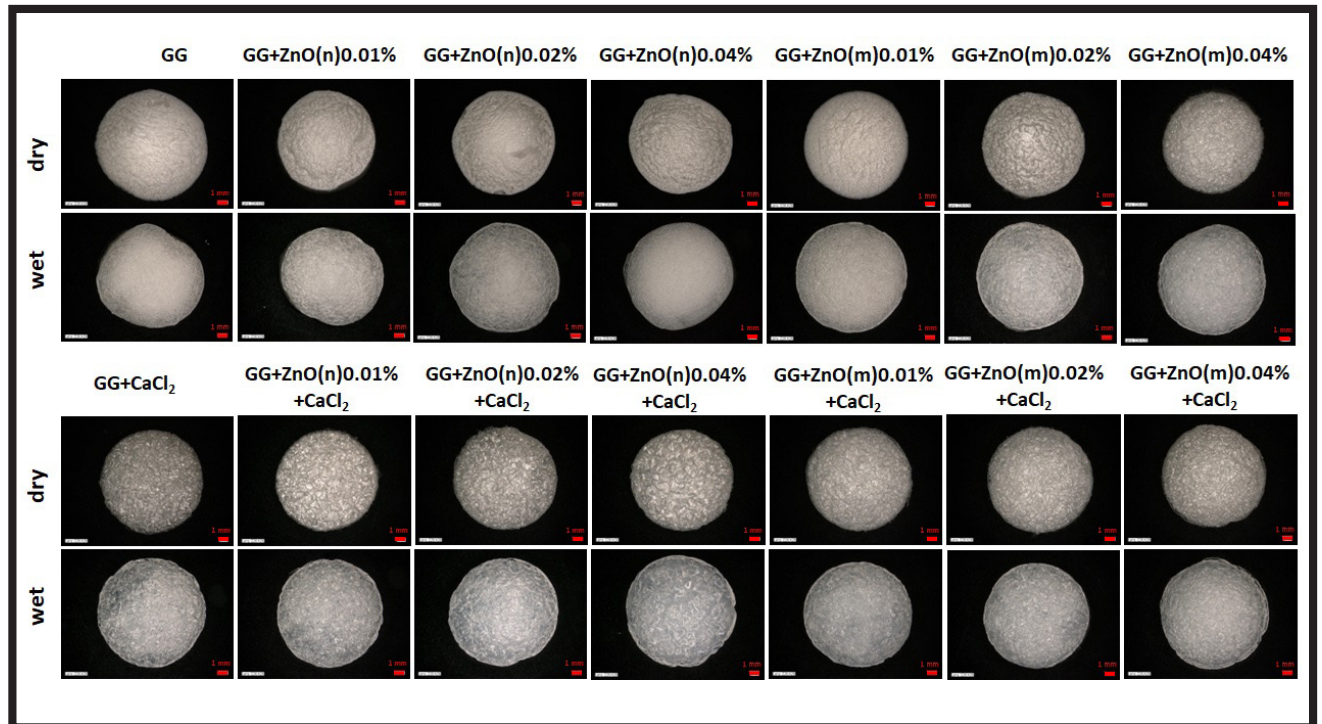


FIG. 1. Pictures of samples after freeze-drying (dry) and after soaking in PBS for 1 h (wet) (Keyence VHX 7000, Belgium, 20x magnification); scale bar = 1 mm.

**TABLE 1. Swelling (after 24 h in PBS), remaining mass (after 48 h in PBS); pH value (after 24 h incubation in UHQ water), and dimensional stability of the samples (after 7 days in UHQ water).**

Sample	Swelling [%]	Remaining mass [%]	pH	Dimensional stability
GG	2500 ± 600	97	5.5	no
GG+ZnO(n)0.01%	3200 ± 100	92	7.5	no
GG+ZnO(n)0.02%	3200 ± 100	94	7.5	no
GG+ZnO(n)0.04%	2950 ± 150	75	7.6	no
GG+ZnO(m)0.01%	2100 ± 200	88	7.5	no
GG+ZnO(m)0.02%	2500 ± 700	92	7.6	no
GG+ZnO(m)0.04%	2250 ± 330	92	7.2	yes
GG+CaCl <sub>2</sub>	3050 ± 400	93	6.1	yes
GG+ZnO(n)0.01%+CaCl <sub>2</sub>	2340 ± 80	98	7.0	yes
GG+ZnO(n)0.02%+CaCl <sub>2</sub>	3900 ± 500	104	7.1	yes
GG+ZnO(n)0.04%+CaCl <sub>2</sub>	3500 ± 400	103	7.3	yes
GG+ZnO(m)0.01%+CaCl <sub>2</sub>	3700 ± 300	87	7.3	no
GG+ZnO(m)0.02%+CaCl <sub>2</sub>	2700 ± 300	98	7.2	yes
GG+ZnO(m)0.04%+CaCl <sub>2</sub>	2900 ± 100	93	7.2	yes

The results obtained show that cross-linked samples with 0.04% ZnO particles (both micrometric and nanometric) and non-cross-linked with 0.04% micrometric ZnO seem to be the most promising for dressings due to their dimensional stability. Hence, they were submitted to further studies to assess zinc release and verify their potential cytotoxicity. For comparison, GG+ZnO(n)0.04%, which was not dimensionally stable and lost the highest amount of mass after incubation, was also tested.

#### Atomic absorption spectrometry

The results of atomic absorption spectrometry results of zinc release after 10 days of incubation in UHQ water for the samples GG+ZnO(n)0.04%, GG+ZnO(m)0.04%, GG+ZnO(n)0.04%+CaCl<sub>2</sub>, and GG+ZnO(m)0.04%+CaCl<sub>2</sub> are shown in FIG. 2. For the above samples, the corresponding zinc concentrations were equal to 2.51 ± 0.04 mg/l, 0.92 ± 0.03 mg/l, 1.94 ± 0.04 mg/l, and 0.93 ± 0.02 mg/l. There was a significantly higher amount of zinc released in the case of the samples with nanometric ZnO compared to that with micrometric ZnO. It may be related to a higher dissolution of ZnO from nanoparticles compared to microparticles due to their higher relative surface area. Crosslinking of the hydrogel with Ca<sup>2+</sup> ions decreased the amount of zinc released from the composites but only in the case of nanometric ZnO particles. No such relationship was found for micrometric ZnO particles, for which zinc release was the lowest. For comparison, GG and GG+CaCl<sub>2</sub> samples were also tested, but zinc, as expected, was not detected in these samples. Our results show that the amount of zinc released should be sufficient to assure antibacterial properties. According to Jayaseelan et al. [13] minimum inhibitory concentrations (MIC) of ZnO nanoparticles against *A. hydrophila*, *E. coli*, *E. faecalis*, *C. albicans* were 1.2, 1.2, 1.5, and 0.9 µg/ml, respectively. According to Ahmed Kadhum [14] the MIC of ZnO nanoparticles against *P. aeruginosa*, *K. pneumoniae*, *E. coli*, *S. aureus*, *S. epidermidis* and *S. pneumoniae* was reported to be 1.25 µg/ml.

#### In vitro cytotoxicity tests

The resazurin reduction test assessing cell viability was carried out for the control sample (L929 cells cultured in the medium, without the addition of extracts) and the hydrogel extracts at a concentration of 0.5% and 1% (FIG. 3). Similar viability was obtained for GG and GG+CaCl<sub>2</sub> samples for both 0.5% and 1% extracts. In the case of the 0.5% and 1% extract for GG, the degree of reduction of Alamar Blue was 45.1 ± 2.5%, 42.0 ± 6.5%, respectively. For the GG+CaCl<sub>2</sub> 0.5% and 1% extracts, it was 48.8 ± 0.1% and 42.3 ± 1.3%, respectively. The control sample showed viability of 66.4 ± 5.9%.

For all samples containing ZnO particles, cell viability was higher in the presence of 0.5% extracts than in the case of 1% extracts. For a non-cross-linked sample containing ZnO nanoparticles (i.e. GG+ZnO(n)0.04%), for which the amount of zinc released was the highest (FIG. 2), and which was also the least stable during incubation (TABLE 1), the viability of the cells was also the lowest.

Interestingly, a level of cell viability comparable to that of the control sample was observed for the samples GG+ZnO(n)0.04%+CaCl<sub>2</sub> and GG+ZnO(m)0.04%+CaCl<sub>2</sub>, i.e., crosslinked with calcium ions, for the 0.5% extract, which were 72.5 ± 6.9% and 74.5 ± 1.6%, respectively. It shows a great potential of CaCl<sub>2</sub> cross-linked samples supplemented with 0.04% ZnO particles for biomedical applications, provided that the concentration of particles and release of zinc are at a defined, not too high level, which is not toxic to cells. For our samples, the highest concentration of zinc released was 2.51 ± 0.04 mg/l for GG+ZnO(n)0.04% sample (FIG. 2). According to the literature, the half-maximum inhibitory concentration (IC50) of ZnO for L929 cells was found to be 50 µg/ml (50 mg/l) [15]. No negative influence of ZnO on HeLa cells was reported for the concentration of ZnO not exceeding 20 mg/l [15].

For 0.5% extracts of GG+ZnO(n)0.04%+CaCl<sub>2</sub> and GG+ZnO(m)0.04%+CaCl<sub>2</sub> samples, there are no statistically significant differences as compared to control.

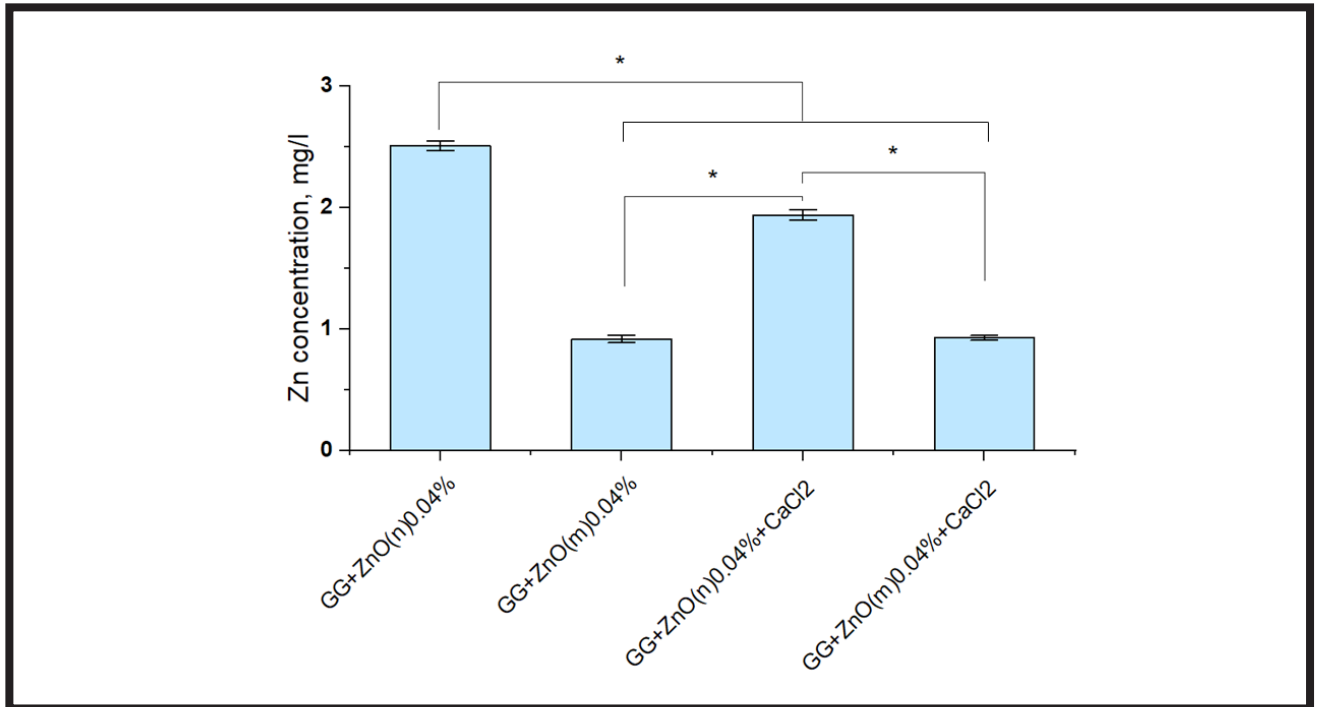


FIG. 2. Zinc concentration in the aqueous medium after immersion of the samples evaluated by atomic absorption spectrometry. Average from  $n = 3$  samples  $\pm$  SD (standard deviation), \* $p < 0.05$ .

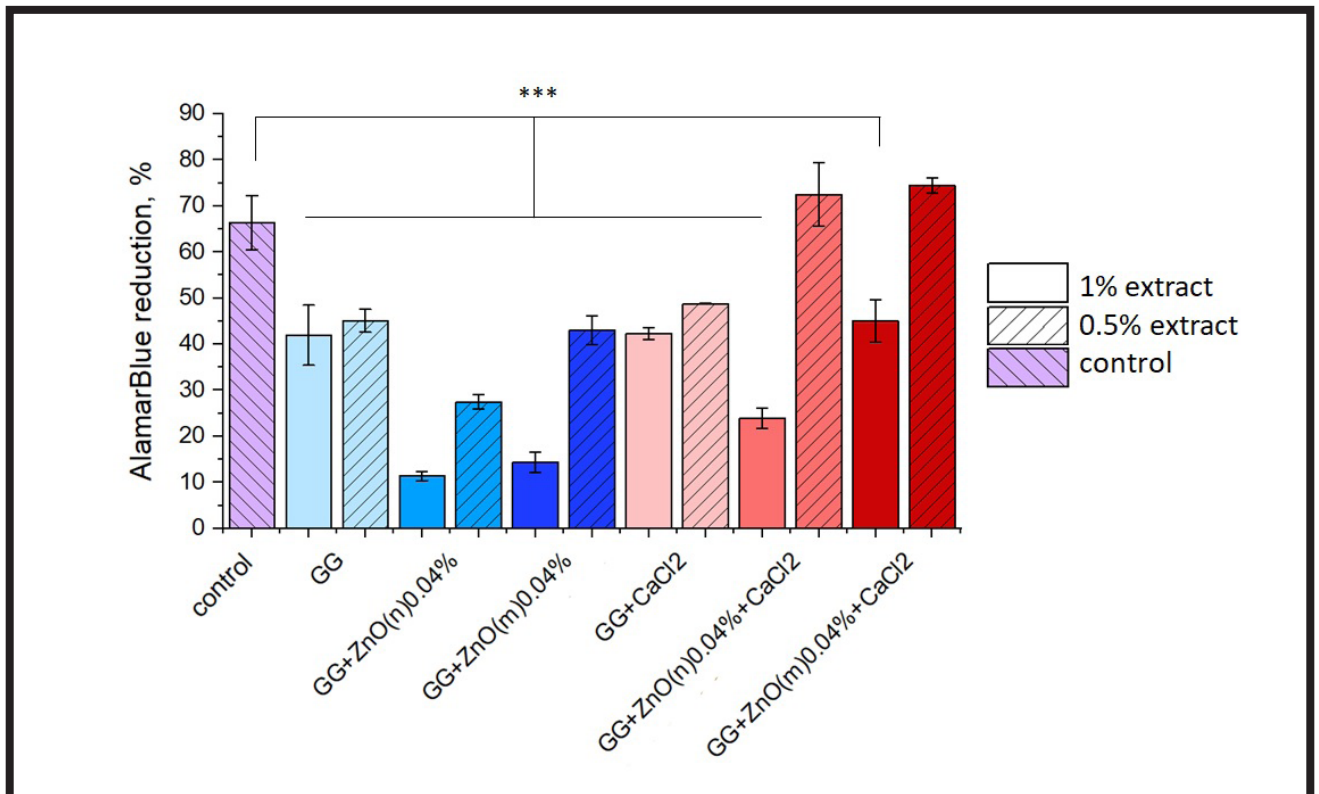


FIG. 3. Viability of L929 cells in contact with 1% and 0.5% extracts from the samples and cells cultured in control conditions (medium without extract addition). Average from  $n = 3$  samples  $\pm$  SD (standard deviation), \*\*\* $p < 0.001$ .

Fluorescence microscopy images of live/dead stained cells cultures in 0.5% and 1% extracts from the samples are shown in FIG. 4.

Live/dead images show the high viability of L929 cells, in particular, for 0.5% hydrogel extracts. The least viable cells are visible in the pictures with 1% hydrogel extracts of GG+ZnO(n)0.04% and GG+ZnO(m)0.04% without the addition of CaCl<sub>2</sub> cross-linker. The results suggest that the absence of this cross-linker caused a greater release of ZnO into the extract, which could have a toxic effect on the cells.

This hypothesis is confirmed by the results of the resazurin reduction test, where the lowest percentage of cell viability was observed in the case of samples not containing CaCl<sub>2</sub>. The 1% extracts were more toxic to cells than the 0.5% extracts, showing that it is possible to reduce the potential cytotoxicity of the materials by reducing the amount of ZnO added and using the particles with micrometric size instead of nanometric size.

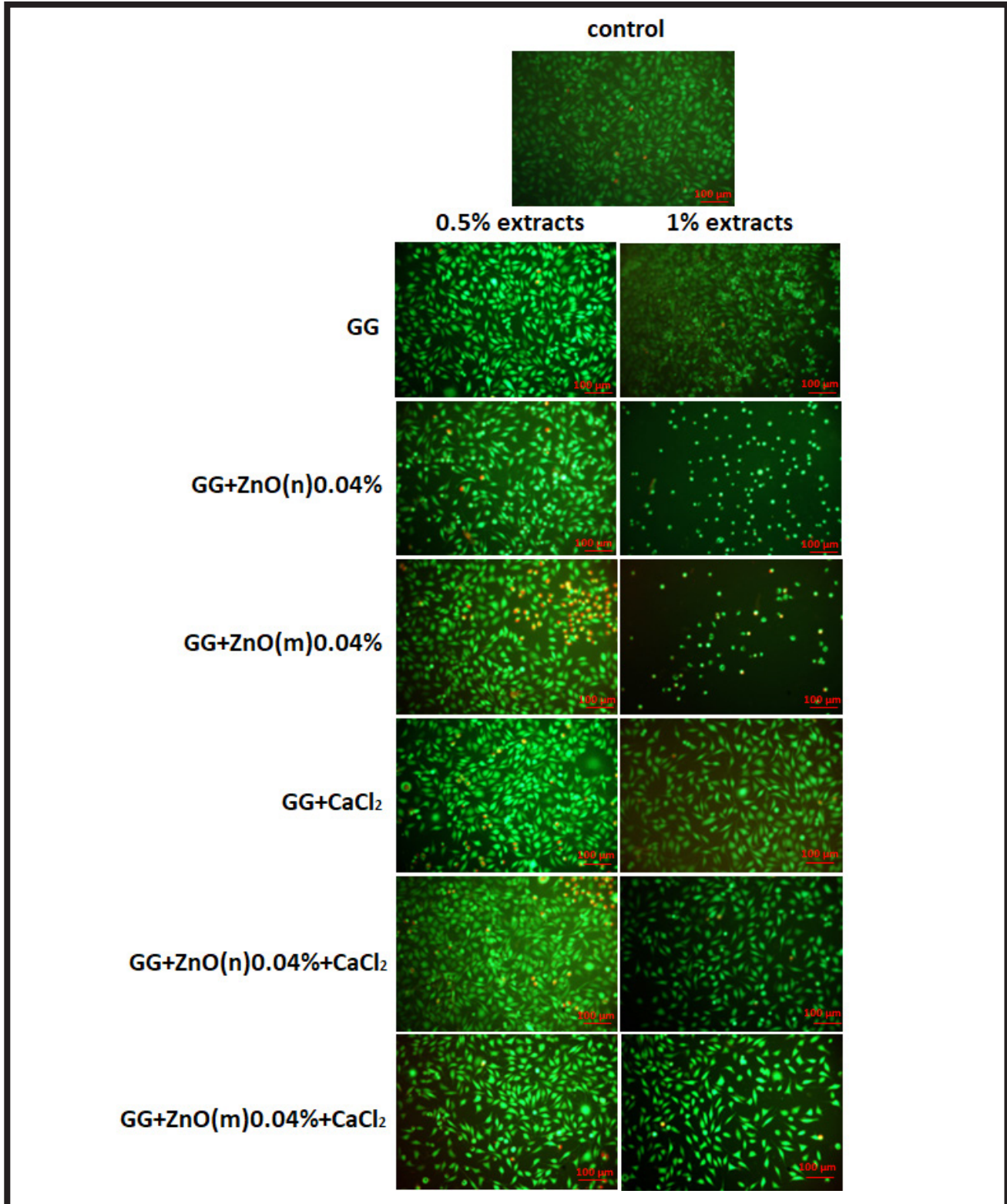


FIG. 4. Live/dead images of L929 cells in contact with 1% and 0.5% extracts from the samples and cells cultured in control conditions (medium without extract addition). Scale bar = 100 μm.

## Conclusions

The study aimed at producing composite hydrogels with the addition of zinc oxide in the form of nanometric and micrometric particles as an antibacterial agent and an additional cross-linker that influences several physicochemical properties of the samples (stiffness, porosity, swelling properties, stability, etc.) and biological performance with L929 fibroblasts.

Microscopic examinations showed a higher porosity of the samples containing  $\text{CaCl}_2$  compared to the samples without this cross-linker. All samples were characterized by high swelling, which is important to ensure absorption of exudates from wounds. Samples with ZnO particles cross-linked with  $\text{CaCl}_2$  lost less mass after incubation in aqueous media and were characterised by better dimensional stability than those without crosslinking. The pH of the extracts of the samples containing ZnO particles was more neutral than that of the control gellan gum samples.

The release of zinc was higher from the samples containing nanometric particles than in the case of micrometric particles. This may be due to an increase in the solubility of ZnO along with a decrease in particle size, because of the higher relative surface area, which resulted in a greater degree of transfer of zinc from the samples to aqueous medium. Interestingly, it was found that zinc release can also be controlled by cross-linking of the gellan gum matrix, because for cross-linked samples containing ZnO nanometric particles, the release of zinc was reduced.

Relatively large amounts of zinc species in the case of samples containing ZnO nanoparticles ( $\text{GG}+\text{ZnO}(\text{n})0.04\%+\text{CaCl}_2$ ) are very promising in the context of antibacterial properties and treatment of infected wounds. The lower amount of zinc released in the case of the samples with ZnO microparticles ( $\text{GG}+\text{ZnO}(\text{m})0.04\%+\text{CaCl}_2$ ) might be sufficient to prevent infection development. Furthermore, both materials show satisfactory cytocompatibility with L929 fibroblasts and durability for at least 7 days under aqueous conditions, paving the way for their use as dressings for infected wounds.

## Acknowledgements

*The authors would like to acknowledge Dr Witold Reczyński for AAS analysis and InPhoCat – Innovative Photocatalytic Solutions Sp. z o.o. for providing zinc oxide samples. This study was supported from the subsidy for AGH University of Krakow (No 16.16.160.557).*

## ORCID iD

A. Macyk: <https://orcid.org/0009-0003-9988-7464>  
 A. Kusibab: <https://orcid.org/0000-0002-5580-7392>  
 E. Pamuła: <https://orcid.org/0000-0002-0464-6189>

## References

- [1] Jia B., Li G., Cao E., Luo J., Zhao X., Huang H.: Recent progress of antibacterial hydrogels in wound dressings. *Mater Today Bio.* 19 (2023) 100582.
- [2] Palumbo F.S., Federico S., Pitarresi G., Fiorica C., Giammona G.: Gellan gum-based delivery systems of therapeutic agents and cells. *Carbohydr Polym.* 229 (2020) 115430.
- [3] Das M., Giri T.K.: Hydrogels based on gellan gum in cell delivery and drug delivery. *J Drug Deliv Sci Technol.* 56 (2020) 101586.
- [4] Gomes D., Batista-Silva J.P., Sousa A., Passarinha L.A.: Progress and opportunities in Gellan gum-based materials: A review of preparation, characterization and emerging applications. *Carbohydr Polym.* 311 (2023) 120782.
- [5] Lee S., Choi J.H., Park A., Rim M., Youn J., Lee W., et al.: Advanced gellan gum-based glycol chitosan hydrogel for cartilage tissue engineering biomaterial. *Int J Biol Macromol.* 158 (2020) 452-460.
- [6] Yu I., Kaonis S., Chen R.: A Study on Degradation Behavior of 3D Printed Gellan Gum Scaffolds. *Procedia CIRP.* 65 (2017) 78-83.
- [7] Gering C., Párraga J., Vuorenperä H., Botero L., Miettinen S., Kellomäki M.: Bioactivated gellan gum hydrogels affect cellular rearrangement and cell response in vascular co-culture and subcutaneous implant models. *Biomater Adv.* 143 (2022) 213185.
- [8] Reczyńska-Kolman K., Hartman K., Kwiecień K., Brzychczy-Włoch M., Pamuła E.: Composites Based on Gellan Gum, Alginate and Nisin-Enriched Lipid Nanoparticles for the Treatment of Infected Wounds. *Int J Mol Sci.* 23(1) (2021) 321.
- [9] Sirelkhatim A., Mahmud S., Seeni A., Kaus N.H.M., Ann L.C., Bakhori S.K.M., et al.: Review on Zinc Oxide Nanoparticles: Antibacterial Activity and Toxicity Mechanism. *Nano-Micro Lett.* 7(3) (2015) 219-242.
- [10] Alshameri A.W., Owais M.: Antibacterial and cytotoxic potency of the plant-mediated synthesis of metallic nanoparticles Ag NPs and ZnO NPs: A review. *OpenNano.* 8 (2022) 100077.
- [11] Ghanbari M., Sadjadinia A., Zahmatkesh N., Mohandes F., Dolatyar B., Zeynali B., et al.: Synthesis and investigation of physicochemical properties of alginate dialdehyde/gelatin/ZnO nanocomposites as injectable hydrogels. *Polym Test.* 110 (2022) 107562.
- [12] Hamid R., Rotshteyn Y., Rabadi L., Parikh R., Bullock P.: Comparison of alamar blue and MTT assays for high through-put screening. *Toxicol In Vitro.* 18(5) (2004) 703-710.
- [13] Jayaseelan C., Rahuman A.A., Kirthi A.V., Marimuthu S, Santhoshkumar T., Bagavan A., et al: Novel microbial route to synthesize ZnO nanoparticles using *Aeromonas hydrophila* and their activity against pathogenic bacteria and fungi. *Spectrochim Acta A Mol Biomol Spectrosc.* 90 (2012) 78-84.
- [14] Ahmed Kadhum S.: The Effect of two Types of Nano-Particles (ZnO and  $\text{SiO}_2$ ) on Different Types of Bacterial Growth. *Biomed Pharmacol J.* 10(4) (2017) 1701-1708.
- [15] Cierech M., Wojnarowicz J., Kolenda A., Krawczyk-Balska A., Prochwicz E., Woźniak B., et al.: Zinc Oxide Nanoparticles Cytotoxicity and Release from Newly Formed PMMA–ZnO Nanocomposites Designed for Denture Bases. *Nanomaterials.* 9(9) (2019) 1318.

# THE PROPERTIES OF FISH COLLAGEN FILMS AFTER CROSS-LINKING WITH TANNIC ACID

ALINA SIONKOWSKA<sup>1\*</sup> , KATARZYNA LEWANDOWSKA<sup>1</sup> ,  
MARTA SZULC<sup>1</sup> , PATRYCJA BRUDZYŃSKA<sup>1</sup> ,  
KAROLINA KULKA<sup>1</sup> , ŁUKASZ PIWOWARSKI<sup>2</sup> 

<sup>1</sup> DEPARTMENT OF CHEMISTRY OF BIOMATERIALS AND COSMETICS, NICOLAUS COPERNICUS UNIVERSITY IN TORUŃ, GAGARINA 7, 87-100 TORUŃ, POLAND

<sup>2</sup> SANCOLL SP. Z O.O., JULIUSZA SŁOWACKIEGO 24, 35-060 RZESZÓW, POLAND

\*E-MAIL: ALINAS@UMK.PL

## Abstract

Over the last three decades, an increasing interest in the preparation of new materials for wound healing has been observed. Collagen is a widely used biomaterial, and especially fish skin collagen is more and more popular among scientists. This study aimed to obtain thin films from native fish skin collagen and collagen cross-linked with tannic acid. Infrared spectroscopy, mechanical test, topographic imaging, and swelling test were used to characterize the features of the mentioned films. Statistical evaluation of the results was conducted with the Q-Dixon test. Infrared spectroscopy analysis showed that in the IR spectra of examined biomaterials, there are slight shifts in band positions after tannic acid cross-linking. The mechanical properties of the cross-linked material were different from those of the native collagen film. The Young's modulus was higher for cross-linked collagen, whereas the elongation at break was lower than for pure collagen. The swelling of the collagen films increased after cross-linking with tannic acid. Swelling tests indicated that collagen cross-linked with tannic acid absorbs more water than before cross-linking. The properties of collagen films were significantly improved after tannic acid cross-linking. All alterations can be a result of collagen cross-linking by tannic acid, probably by forming hydrogen bonds between collagen and tannic acid.

**Keywords:** collagen, biomaterials, medicine, wound dressing, cross-linking, tannic acid

## Introduction

Collagen is the most abundant protein in the human body and plays an important role in providing strength and maintenance the right structure of tissues, as well as creating a scaffold for internal organs [1-3]. Currently, 29 genetically different collagen types are known [4], however, the most commonly used in medical applications is type I collagen. In recent years, an increase in the application of fish skin collagen increased [5,6]. It is the result of the transition of several diseases from mammals and also due to some religious aspects existing in some regions of the world.

[Engineering of Biomaterials 168 (2023) 9-14]

doi:10.34821/eng.biomat.168.2023.9-14

Submitted: 2023-04-06, Accepted: 2023-05-08, Published: 2023-05-12



Copyright © 2023 by the authors. Some rights reserved.  
Except otherwise noted, this work is licensed under  
<https://creativecommons.org/licenses/by/4.0>

The attention is mainly focused on fish waste, which makes up about 50-70% of seafood production [7-8]. Collagen can be extracted not only from the fish skin, but also from heads, scales, bones, fins, air bladders, and other entrails [8]. Fish collagen has a significantly lower denaturation temperature in comparison to mammalian collagen due to the lower hydroxyproline content [9,10], but collagen extracted from silver carp (*Hypophthalmichthys molitrix*) shows a quite high denaturation temperature in contrast to other fish species [10]. To improve the stability and mechanical properties of collagen, several cross-linking methods can be used [11-19].

Glutaraldehyde is one of the chemical compounds often used to improve the mechanical properties of collagen-based biomaterials [12,13]. Next, genipin is also widely applied for collagen cross-linking [14,15]. This compound is much less toxic than glutaraldehyde and other commonly used cross-linking agents.

The chemical cross-linking of collagen can be performed using 1-Ethyl-3-(3-dimethylaminopropyl) carbodiimide (EDC) and N-hydroxysuccinimide (NHS) [16,17]. This method of cross-linking of collagen leads to the formation of a covalent bond between the carboxylic acid groups from aspartic and glutamic acid. Another cross-linking agent used for collagen modification is dialdehyde starch (DAS).

DAS was used as a cross-linking agent for collagen [18] and gelatin [19] to improve the properties of the materials. DAS aldehyde groups interact with a free amino group of collagen during the cross-linking reaction. As a result, collagen can be intra- and intermolecularly linked via DAS bridges.

Chemical cross-linking is crucial for collagen properties because collagen-based materials are widely used in biomedical and cosmetic industries [20]. It may influence collagen properties for wound healing applications [21-23]. Collagen hydrogels can also be loaded with other active substances making up the base of various kinds of cosmetic products, e.g. beauty masks.

In this work, collagen from the skin of Silver carp was cross-linked with tannic acid and the properties of collagen materials were studied. Based on the results of our previous research on the cross-linking of biopolymers, we assumed that it can improve the collagen properties important for medical applications [24-26]. Despite the level of development of collagen-based wound dressings attained so far, there is still a pressing need for further improvements.

## Materials and Methods

### Materials and film preparation

Collagen (Col) from skins of Silver carp fish was purchased from SanColl Sp. z o.o., Poland. Acetic acid was purchased from Avantor Performance Materials, Poland. The solution of 0.4 M acetic acid solution was prepared by diluting concentrated acetic acid with distilled water. To obtain a 1% solution, collagen was dissolved in the previously prepared solvent. For cross-linking of collagen, 1% and 2% of tannic acid were added and the solution was mixed for 2 hours. Thin films were obtained by pouring 25 g of each solution onto plastic plates with dimensions 100 x 100 x 20 mm.

### FTIR spectroscopy

The interactions between the polymer and the additive were evaluated by Fourier transform infrared spectroscopy using Nicolet iS10 equipment with an ATR accessory and a diamond crystal (Thermo Fisher Scientific, Waltham, MA, USA). For all spectra, 64 scans were recorded in absorption mode, with a resolution of 4 cm<sup>-1</sup>. OMNIC 9 software was used to edit the spectra.

### Mechanical properties

Mechanical tests were carried out using a mechanical testing machine (Z.05, Zwick and Roell, Ulm, Germany). Young's modulus, tensile strength, and elongation at break were evaluated. Samples were cut in the shape of paddles (width 4 mm in the center). Testing program parameters were as follows: the speed starting position was 50 mm/min, the speed of the initial force was 5 mm/min, and the initial force was 0.1 MPa. Data were collected using the TestXpert II 2017 program, and results were presented as average values with standard deviation.

### Scanning electron microscopy (SEM-EDX)

Surface imaging of the tested polymer samples was carried out using a scanning electron microscope manufactured by LEO Electron Microscopy Ltd. (Model 1430 VP). In addition, an EDX Quantax 200 X-ray spectrometer with a Bruker AXS XFlash 4010 detector was used for spot analysis of the chemical composition of the samples to confirm the presence of zinc.

### Atomic force microscopy (AFM)

The microstructure of the polymer samples was analyzed using atomic force microscope images obtained by Multi-Mode Scanning probe microscope NanoScope IIIa (Digital Instruments Veeco Metrology Group, Santa Barbara, CA).

### Swelling measurements

The swelling ratio was measured by immersing the composite fragments in phosphate buffered saline (PBS) solution, pH = 7.4, and citric buffer at pH 5.5. After 1, 2, 4, 8, 12, 24, and 48 hours of immersion, the materials were gently dried by putting them between two sheets of paper and then weighed [27]. The swelling ratios were calculated using the following equation:

$$\text{swelling} = \frac{(m_t - m_0)}{m_0} \cdot 100\% [\%]$$

$m_t$  - weight of the material after immersion in PBS [mg],  
 $m_0$  - weight of the material before immersion [mg].  
 Samples of each type were measured in triplicate.

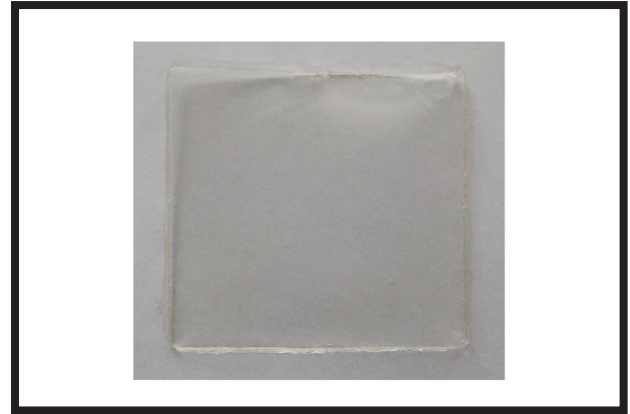


FIG. 1. An example of a film made from fish collagen.

## Results and Discussions

### Collagen films

After solvent evaporation, we obtained collagen film that could be removed easily from plastic plates. The example of obtained collagen film is presented in FIG. 1. The fish collagen film is translucent and mat. Collagen films cross-linked with tannic acid looked very similar.

### FTIR spectroscopy analysis

For pure collagen films and collagen cross-linked with tannic acid, infrared spectroscopy analysis was done. IR spectra of the examined biomaterials are presented in FIG. 2.

FIG. 2 shows the FTIR spectra of collagen films before and after cross-linking with tannic acid. In general, the positions of the main bands in the IR spectra are the same. The analysis showed that the amide I peak observed in fish collagen at  $1634 \text{ cm}^{-1}$  after cross-linking with tannic acid can be found at  $1631 \text{ cm}^{-1}$ .

The amide II peak appears at  $1544 \text{ cm}^{-1}$  in collagen spectra, whereas after cross-linking it was found at  $1542 \text{ cm}^{-1}$ . The amide III peak characteristic for collagen appears in the spectra of collagen and cross-linked collagen at about  $1450 \text{ cm}^{-1}$ . In the range between  $2000 \text{ cm}^{-1}$  to  $4000 \text{ cm}^{-1}$ , all studied samples showed absorbance due to the presence of amide A and hydroxyl groups.

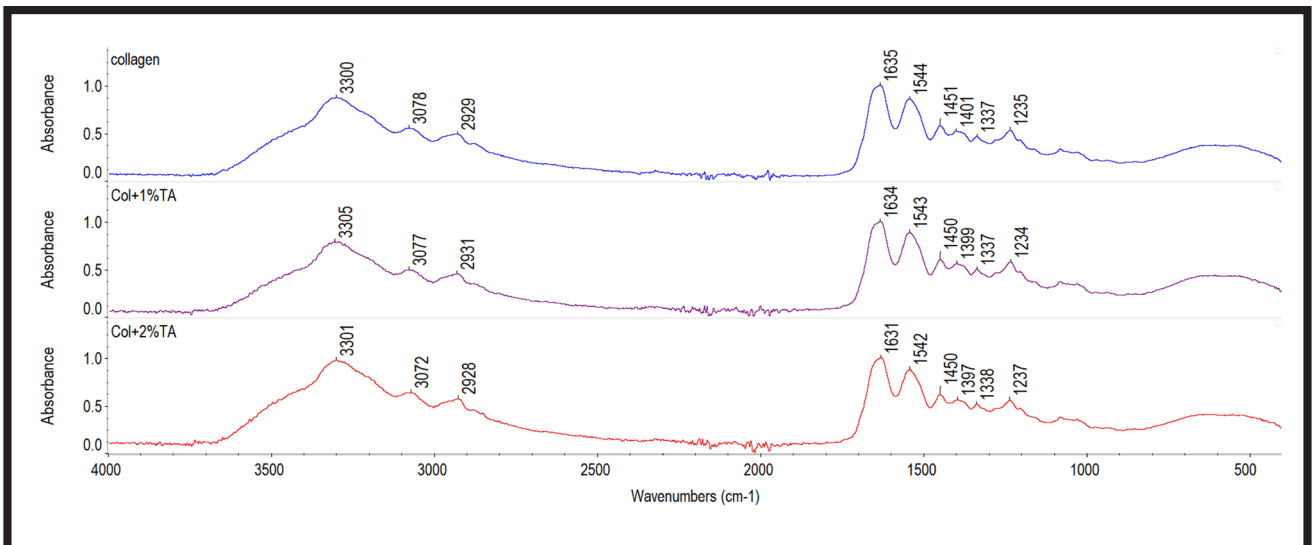


FIG. 2. FTIR spectra of films made of non-cross-linked collagen films and collagen films cross-linked with tannic acid.

The analysis indicated that in the IR spectra of cross-linked collagen the amide A was shifted to lower wavenumbers. The amide B peaks are in the same position before and after cross-linking of collagen.

The small changes observed in the peak positions may show that the addition of tannic acid influences the interactions between collagen macromolecules, which are mainly via hydrogen bonds. Hydrogen bonds can be formed between collagen molecules and also between collagen and tannic acid molecules.

**Mechanical properties**

For each film obtained in this research, mechanical properties were measured. The results are shown in FIGs. 3-5.

The results of the mechanical properties measurements indicated that the film made of collagen from fish skin showed a lower Young's modulus than those cross-linked with tannic acid (FIG. 4). The film with a 2% content of tannic acid showed the highest Young's modulus in this research.

However, with increasing amounts of tannic acid, the elasticity of the films decreased (FIG. 5). It can be assumed that after cross-linking of fish collagen with tannic acid, the flexibility of the films is smaller. For medical applications such as wound dressing, mechanical properties are crucial because they decide about the possibility of application without destroying. The values of standard deviation may indicate that the films absorb the humidity that is present in the laboratory during the measurements, which could further change their properties. However, the values of mechanical properties are good enough for the applications mentioned above. Nevertheless, another cross-linking agent should also be considered in the future.

**Topography imaging**

The image of the surface topography and the surface structure of the studied collagen thin film is presented below (FIG. 6). The value of the surface roughness for collagen film was about 8 nm when we consider the Rq value. The structure of the surface observed by AFM for cross-linked collagen films was similar.

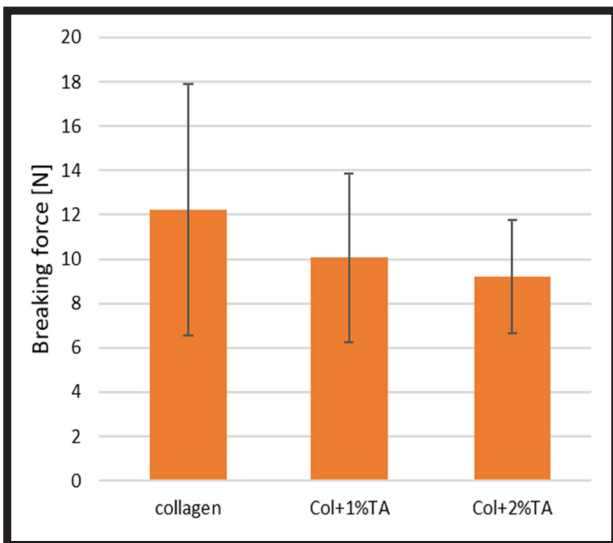


**FIG. 3.** The breaking force for non-cross-linked collagen films and collagen films cross-linked with tannic acid.

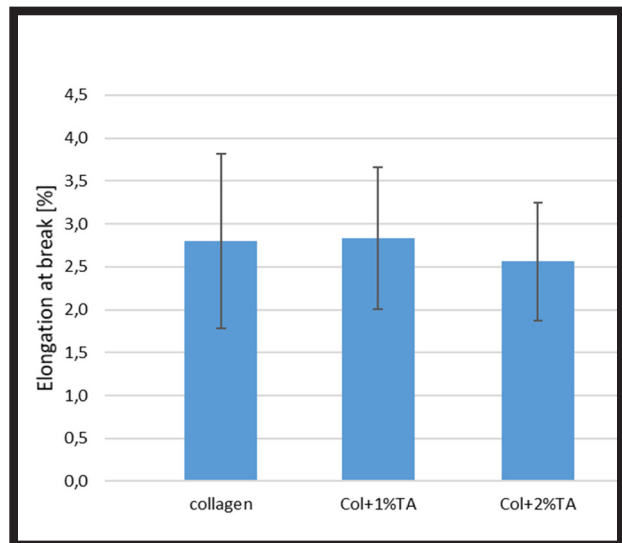


**FIG. 5.** The elongation at break for non-cross-linked collagen films and collagen films cross-linked with tannic acid.

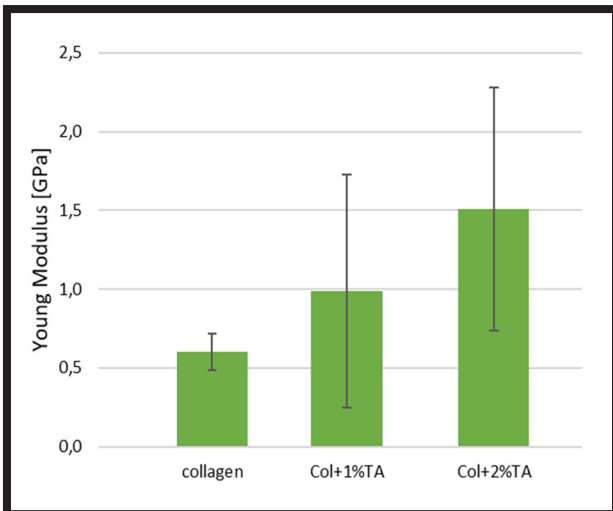


**FIG. 4.** Young modulus for non-cross-linked collagen films and collagen films cross-linked with tannic acid.

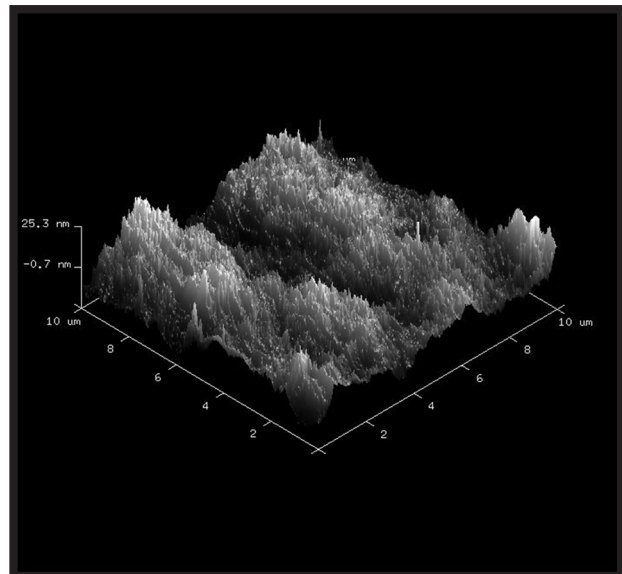


**FIG. 6.** AFM image of the fish collagen thin film.

### Swelling test

Pictures of thin film samples in PBS solution after soaking for several periods are presented below (FIG. 7). The degree of swelling in PBS solution and citric buffer solution (pH 5.5) is shown in FIG. 8 and FIG. 9, respectively.

Swelling tests indicated that all samples absorb water and are stable even after 48 hours. However, after 8 hours of soaking in PBS solution citric buffer, all samples fell apart while being removed from the solution. Only films made of collagen cross-linked with tannic acid remained integral for up to 8 hours. The degree of swelling is greater for collagen cross-linked with tannic acid.

Materials made of collagen and collagen cross-linked with tannic acid were easily wettable by polar solvents such as PBS and/or citric buffer. All materials prepared in this research showed high swelling ability. This is because collagen contains a large number of functional groups capable of binding water [27-29]. The PBS solution with pH = 7.4 may correspond to the pH of blood, so the swelling in this pH can be crucial from a practical point of view. For healthy skin, the pH is about 5.5, so in this research, the swelling properties were also measured in a citric buffer in the above-mentioned pH to compare the swelling behavior in two different pH.

Although the biocompatibility test was not performed in this research, we have previously found, that cross-linking of biopolymer blends with tannic acid leads to biocompatible materials [26,30].

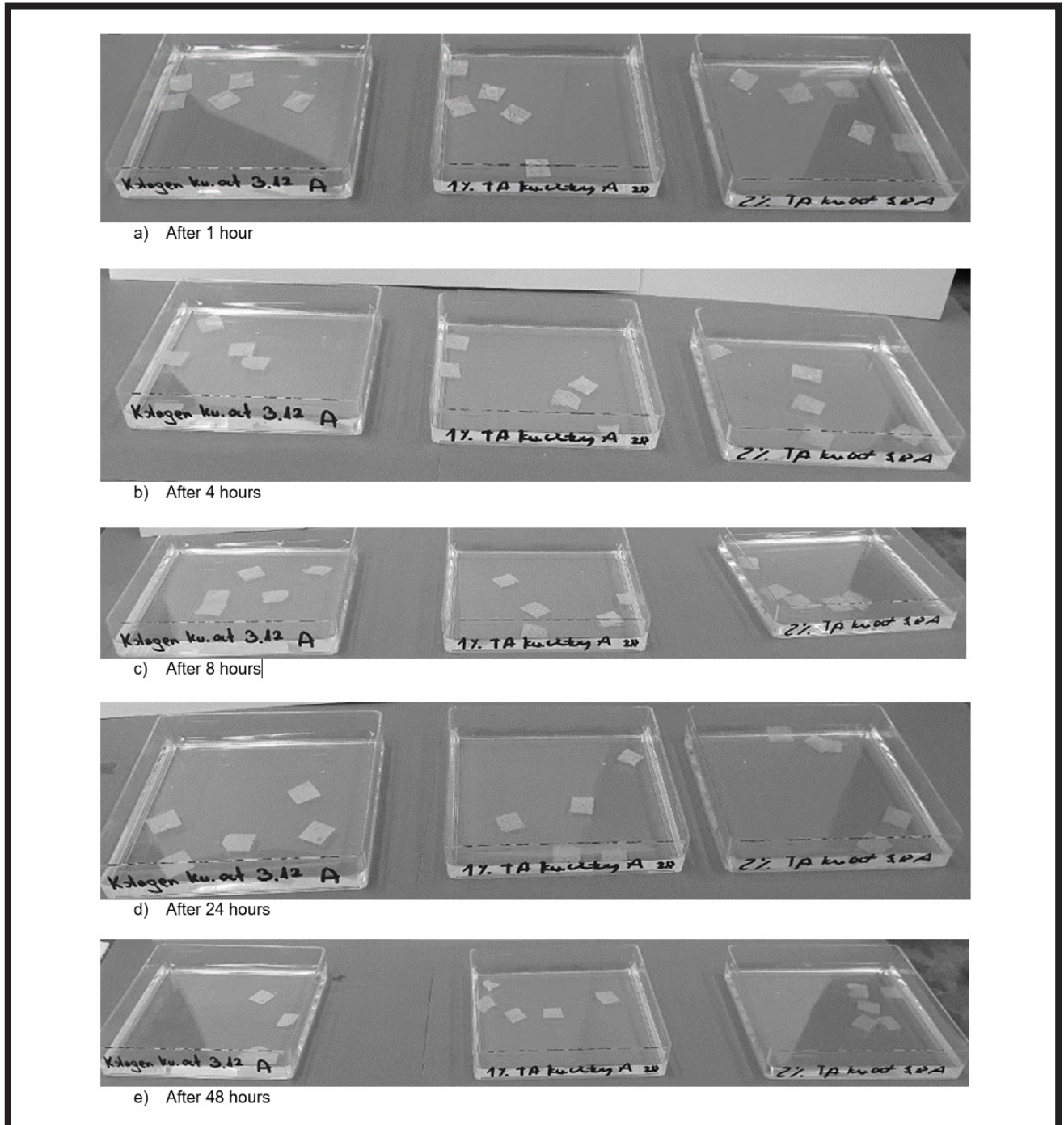


FIG. 7. Swelling of collagen films in PBS (from the left: non-cross-linked collagen, collagen + 1% of tannic acid, collagen + 2% of tannic acid).

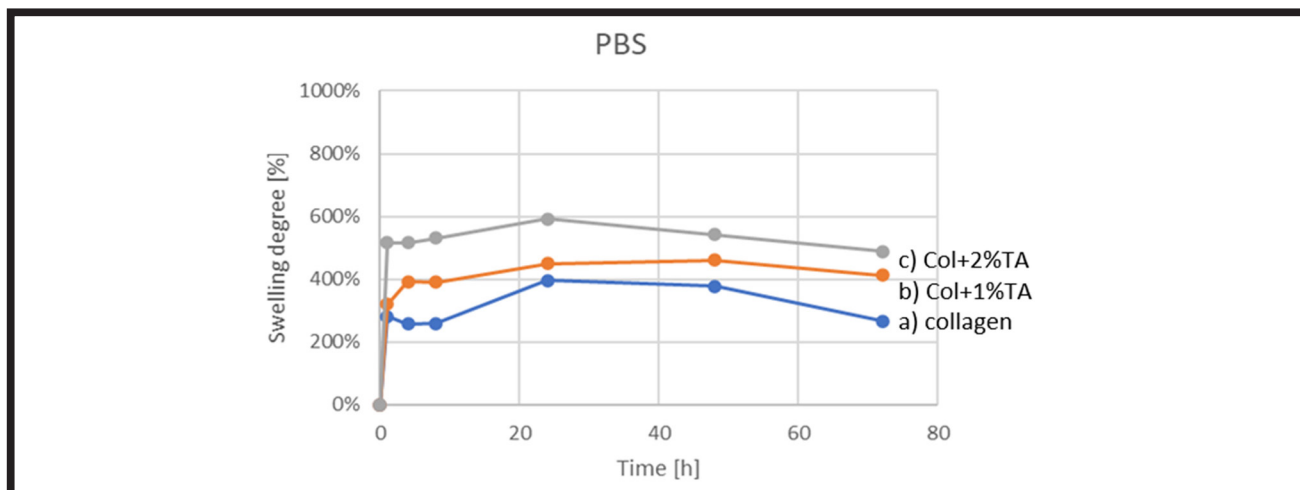


FIG. 8. Swelling of collagen films in PBS: a) non-cross-linked collagen; b) collagen + 1% of tannic acid; c) collagen + 2% of tannic acid.

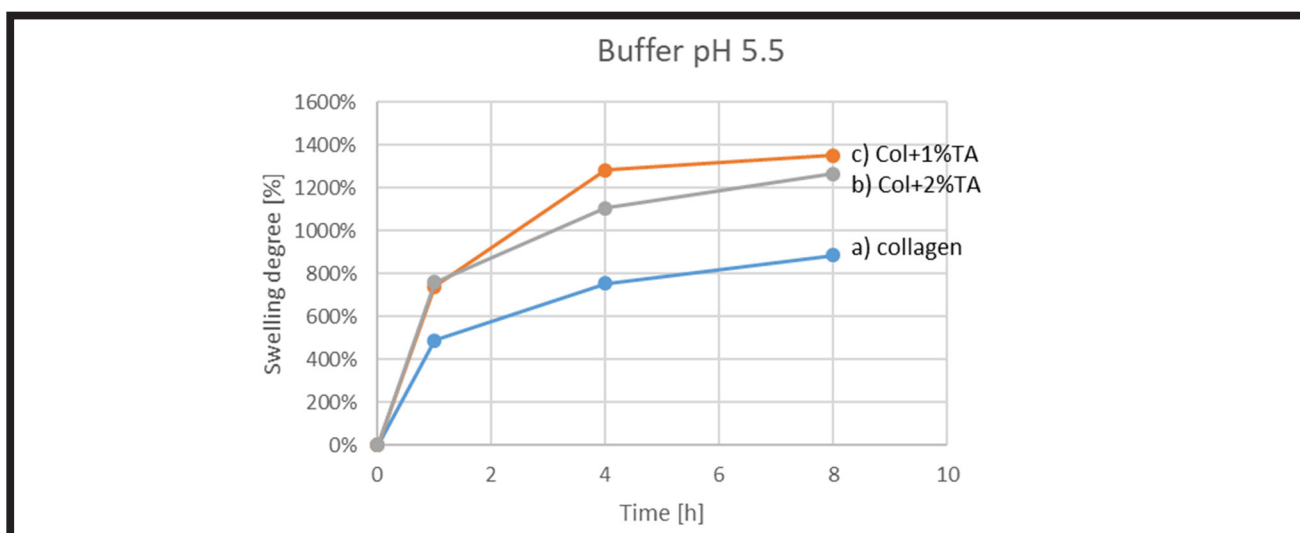


FIG. 9. Swelling of collagen films in citric buffer (pH 5.5): a) non-cross-linked collagen; b) collagen + 1% of tannic acid; c) collagen + 2% of tannic acid.

## Conclusions

The addition of tannic acid to fish skin collagen leads to alterations in mechanical and swelling properties. These properties are crucial for application in wound dressing. Young's modulus was higher for cross-linked collagen, whereas the elongation at break was smaller than that for non-cross-linked collagen. The swelling of collagen films increased after cross-linking with tannic acid. The swelling tests indicated that collagen cross-linked with tannic acid absorbs more water than the non-cross-linked material, which may suggest also better absorption of exudate from the wound. To sum up, the properties of films made of fish skin collagen improved slightly after tannic acid cross-linking. The alterations can be a result of collagen cross-linking by tannic acid probably by forming hydrogen bonds. The slight shifts in the amide bands confirm the alterations in hydrogen bonding in collagen macromolecules. As there is still a need for the development of collagen-based wound dressings, our results may show a simple way for further improvements of these dressings and may encourage further research. However, other cross-linking agents should also be investigated in the future for further improvement of fish collagen materials.

## Acknowledgements

The authors acknowledge SanColl company for preparing fish skin collagen for this research.

The research was funded by NCBiR (grant number POIR.04.01.04-00-0077/20-00).

## ORCID iD

A. Sionkowska: <https://orcid.org/0000-0002-1551-2725>  
 K. Lewandowska: <https://orcid.org/0000-0002-8380-4009>  
 M. Szulc: <https://orcid.org/0000-0003-2398-8616>  
 P. Brudzyńska: <https://orcid.org/0000-0002-6646-1534>  
 K. Kulka: <https://orcid.org/0000-0002-0825-1774>  
 Ł. Piwowarski: <https://orcid.org/0009-0000-6889-9209>

## References

- [1] Mohan S., Oluwafemi O.S., Kalarikkal N., Thomas S., Songca S.P.: *Biopolymers – Application in Nanoscience and Nanotechnology* (2016). London: IntechOpen.
- [2] Gaspar-Pintilieșcu A., Stanciu A.M., Craciunescu O.: Natural composite dressings based on collagen, gelatin and plant bioactive compounds for wound healing: A review. *International Journal of Biological Macromolecules* 138 (2019) 854–865.
- [3] Avila Rodríguez M.L., Rodríguez Barroso L.G., Sánchez M.L.: Collagen: A review on its sources and potential cosmetic applications. *Journal of Cosmetic Dermatology* 17 (2018) 20–26.
- [4] Sionkowska A.: Collagen blended with natural polymers: Recent advances and trends. *Progress in Polymer Science* 122 (2021) 101452.
- [5] Zhang J., Duan R., Tian Y., Konno K.: Characterisation of acid-soluble collagen from skin of silver carp (*Hypophthalmichthys molitrix*). *Food Chemistry* 116 (2009) 318–322.
- [6] Liu D., Zhou P., Li T., Regenstein J.M.: Comparison of acid-soluble collagens from the skins and scales of four carp species. *Food Hydrocolloids* 41 (2014) 290–297.
- [7] Faralizadeh S., Rahimabadi E.Z., Bahrami S.H., Hasannia S.: Extraction, characterization and biocompatibility evaluation of collagen from silver carp (*Hypophthalmichthys molitrix*) skin by-product. *Sustainable Chemistry and Pharmacy* 22 (2021)
- [8] Sionkowska A., Adamiak K., Musial K., Gadomska M.: Collagen based materials in cosmetic applications: A review. *Materials* 13 (2020) 1–15.
- [9] Sionkowska A., Lewandowska K., Adamiak K.: The influence of uv light on rheological properties of collagen extracted from silver carp skin. *Materials* 13 (2020) 1–10.
- [10] Guillerme J.B., Couteau C., Coiffard L.: Applications for marine resources in cosmetics. *Cosmetics* 4 (2017) 1–15.
- [11] Adamiak K., Sionkowska A. *Current Methods of Collagen Cross-linking: Review*. *Inter. Journal Biol. Macromol.* 161 (2020) 550-560.
- [12] Jastrzębska M., Wrzaliak R., Kocot. A., Zalewska-Rejda J., Cywilna B.: Raman spectroscopic study of glutaraldehyde – stabilized collagen and pericardium issue, *J. Biomater. Sci., Polym. Ed.* 14 (2003) 185-197.
- [13] Migneault I., Dartiguenave C., Bertrand J., Waldron K.: Glutaraldehyde: behavior in aqueous solution, reaction with proteins, and application to enzyme crosslinking. *Biotechniques* 37 (2004) 790-802.
- [14] Butler M.F., Ng Y.F., Pudney P.D.: Mechanism and kinetics of the crosslinking reaction between biopolymers containing primary amine groups and genipin, *J. Polym. Sci. Pol. Chem.* 41 (2003) 3941-3953.
- [15] Mu C., Zhang K., Lin W., Li D.: Ring-opening polymerization of genipin and its long-range crosslinking effect on collagen hydrogel. *J. Biomed. Mater. Res. A* 101 (2013) 385-393.
- [16] Yang C.: Enhanced physicochemical properties of collagen by using EDC/NHS-crosslinking. *Bull. Mater. Sci.* 35 (2012) 913-918.
- [17] Goodarzi H., Jadidi K., Pourmotabed S., Sharifi E., Aghamollaei H.: Preparation and in vitro characterization of cross-linked collagen-gelatin hydrogel using EDC/NHS for corneal tissue engineering applications. *Int. J. Biol. Macromol.* 126 (2019) 620-632.
- [18] Mu C., Liu F., Cheng Q., Li H., Wu B., Zhang G., Lin W.: Collagen cryogel cross-linked by dialdehyde starch, *Macromol. Mater. Eng.* 295 (2010) 100-107.
- [19] Martucci J., Ruseckaite R.: Tensile properties, barrier properties, and biodegradation in soil of compression: molded gelatin-dialdehyde starch films. *J. Appl. Polym. Sci.* 112 (2009) 2166-2178.
- [20] Sionkowska A., Skrzyński S., Śmiechowski K., Kołodziejczak A.: The review of versatile application of collagen. *Polym Adv. Technol.* 28 (2017) 4-9.
- [21] Guerra A., Belinha J., Jorge R.N.: Modelling skin wound healing angiogenesis: A review. *Journal of Pharmaceutical and Biomedical Analysis* 163 (2019) 1-17.
- [22] Boateng J., Catanzano O.: Advanced therapeutic dressings for effective Wound healing - a review. *J Pharm Sci Elsevier Masson SAS.* 104 (2015) 3653-3680.
- [23] Sorg H., Tilkorn D.J., Hager S., Hauser J., Mirastschijski U.: Skin Wound healing: an update on the current knowledge and concepts. *Eur Surg Res.* 58 (2017) 81-94.
- [24] Kaczmarek B., Sionkowska A.: Scaffolds based on chitosan and collagen with glycosaminoglycans cross-linked by tannic acid. *Polymer Testing* 65 (2018) 163-168.
- [25] Mitura S., Sionkowska A., Jaiswal A.: Biopolymers for hydrogels in cosmetics: review. *Journal of Materials Science: Materials in Medicine* 43 (2020) 31:50.
- [26] Kaczmarek B., Nadolna K., Owczarek A., Michalska-Sionkowska M., Sionkowska A.: The characterization of thin films based on chitosan and tannic acid mixture for potential applications as wound dressings. *Polymer Testing* 78 (2019) 106007.
- [27] Sionkowska A., Grabska S., Lewandowska K., Andrzejczyk A.: Polymer films based on silk fibroin and collagen - the physicochemical properties. *Mol Cryst Liq Cryst* 640 (2016) 13-20.
- [28] Sionkowska A., Grabska S.: Preparation and characterization of 3D collagen materials with magnetic properties. *Polym Test* 62 (2017) 382-391.
- [29] Sionkowska A., Grabska S.: Incorporation of magnetite particles in 3D matrices made from the blends of collagen, chitosan, and hyaluronic acid. *Adv Polym Technol* 37 (2018) 1–10.
- [30] Kaczmarek B., Sionkowska A.: Scaffolds based on chitosan and collagen with glycosaminoglycans cross-linked by tannic acid. *Polymer Testing* 65 (2018) 163-168.

# CURCUMIN DELIVERY SYSTEMS AS DRESSING COMPONENTS FOR THE TREATMENT OF DIABETIC FOOT ULCERS: TESTS ON MACROPHAGES POLARIZATION

KAROLINA WÓJCIK<sup>1\*</sup> , ANNA KUSIBAB<sup>1</sup> , ANA BEATRIZ SOUSA<sup>2,3,4</sup> , JUDITE NOVAIS BARBOSA<sup>2,3,4</sup> , ELŻBIETA PAMUŁA<sup>1</sup> 

<sup>1</sup> AGH UNIVERSITY OF KRAKOW, FACULTY OF MATERIALS SCIENCE AND CERAMICS, DEPARTMENT OF BIOMATERIALS AND COMPOSITES, AL. A. MICKIEWICZA 30, 30-059 KRAKOW, POLAND  
<sup>2</sup> I3S – INSTITUTO DE INVESTIGAÇÃO E INOVAÇÃO EM SAÚDE, UNIVERSIDADE DO PORTO, RUA ALFREDO ALLEN 208, 4200-135 PORTO, PORTUGAL  
<sup>3</sup> INEB – INSTITUTO DE ENGENHARIA BIOMÉDICA, UNIVERSIDADE DO PORTO, RUA ALFREDO ALLEN 208, 4200-135 PORTO, PORTUGAL  
<sup>4</sup> INSTITUTO CIÊNCIAS BIOMÉDICAS ABEL SALAZAR DA UNIVERSIDADE DO PORTO, RUA DE JORGE VITERBO FERREIRA 228, 4050-313 PORTO, PORTUGAL  
 \*E-MAIL: KAROLINA.WOJCIK1@INTERIA.PL

## Abstract

The natural wound healing process consists of four basic phases: homeostasis, inflammation, proliferation, and remodelling. Macrophages play an important role in the body's response to biomaterials, as they are modulators of the wound healing process and can polarize into different phenotypes capable of inducing both deleterious and beneficial effects on tissue repair. Curcumin (CU) is known for its anti-inflammatory properties and has the potential to treat diabetic foot ulcers, but it should be delivered to wounds in a controlled manner. In this study, the encapsulation of curcumin in polymeric microparticles based on poly(sebacic anhydride) (PSA) was developed using an emulsification method. PSA-based microparticles containing different concentrations of CU were obtained: 0% weight (wt). CU (unloaded microparticles), 5, 10, and 20 wt% CU. CU encapsulation efficiency and loading were determined using a fluorescence-based calibration curve method and semi-quantitative Fourier-transform infrared spectroscopy (FTIR) analysis. The potential cytotoxicity of the obtained biomaterials in contact with primary human macrophages and their susceptibility to polarization from the M1 (pro-inflammatory) phenotype to the M2 (anti-inflammatory) phenotype were evaluated. The morphology of cells cultured in contact with polymeric microparticles was evaluated using phalloidin red and 4',6-diamidino-2-phenylindole (DAPI) staining. Macrophage phenotype was assessed using flow cytometry. The obtained biomaterials showed no cytotoxic effect on primary human macrophages.

[Engineering of Biomaterials 168 (2023) 15-24]

doi:10.34821/eng.biomat.168.2023.15-24

Submitted: 2023-04-25, Accepted: 2023-05-12, Published: 2023-05-18



Copyright © 2023 by the authors. Some rights reserved. Except otherwise noted, this work is licensed under <https://creativecommons.org/licenses/by/4.0>

Flow cytometry studies showed enhanced polarization of macrophages into anti-inflammatory M2 phenotype when exposed to microparticles loaded with CU and CU powder as compared to unloaded microparticles.

**Keywords:** curcumin, immunomodulation, inflammation, macrophage polarization, polymeric microparticles, wound healing

## Introduction

Diabetes mellitus is a chronic disease characterized by hyperglycemia that can lead to various complications, such as diabetic wounds and ulcers. These complications require long-term treatment and negatively affect the patient's quality of life [1]. High and persistent glucose levels can cause vascular damage, which can affect and harm nerves, leading to neuropathy that may cause severe damage, resulting in serious infections and ulcers [2].

According to epidemiological studies by the International Diabetes Federation (IDF), around 463 million people suffered from diabetes in 2019, and this number is estimated to increase to 578 million in 2030 and 700 million in 2045, with 20% of the patients developing diabetic wounds [3]. Another study showed that 3.1-11.8% of patients with diabetes have foot ulcers and are 10-20 times more likely to suffer a lower limb amputation [4]. In addition, diabetic foot ulcers are known to affect patients economically, as their healthcare costs are 5 times higher than those of diabetic patients without foot ulcers [5]. Diabetes complicates and prolongs the natural wound-healing process, as it stops it in the inflammatory phase [6]. Impaired function and decreased neutrophil infiltration lead to oxidative stress and the release of pro-inflammatory cytokines. Prolonged exposure to reactive oxygen species (ROS) causes cellular dysfunction and destructive oxidation of intracellular lipids, nucleic acids, and proteins. Peroxisome proliferator-activated receptor (PPAR $\gamma$ ) expression is dysregulated in normal wound healing facilitating the transition of macrophages from an M1 (pro-inflammatory) to an M2 (anti-inflammatory) like phenotype, critical for normal wound healing [7].

Macrophages are key modulators of the wound healing process as they play a unique role in ensuring proper healing. Initially, pro-inflammatory macrophages (M1) infiltrate after injury to clear the wound of bacteria, foreign debris, and dead cells. In acute wounds, as the tissue begins to repair, the overall macrophage population transitions to the M2 phenotype that promotes anti-inflammatory effects and the migration and proliferation of fibroblasts, keratinocytes, and endothelial cells to restore the dermis, epidermis, and vasculature [8]. Moreover, macrophages express growth factors and cytokines essential for angiogenesis, cell proliferation, and extracellular matrix deposition [9]. Eventually, the wound closes and a scar forms. Early in the final phase of the remodeling phase, macrophages release matrix metalloproteinases (MMPs) to degrade the provisional extracellular matrix, and then apoptose so that the skin can mature to its original intact state [8]. The macrophage phenotype gradually changes throughout the healing process from an initial pro-inflammatory M1 phenotype characteristic of the acute response to a pro-regenerative M2 phenotype that allows accurate tissue repair [9]. In chronic wounds, pro-inflammatory macrophages persist without transitioning to anti-inflammatory phenotypes; which is thought to contribute to the impairment in tissue repair [8].

Nanotechnology-based therapies have emerged as a promising treatment for chronic diabetic foot ulcers, due to their unique properties and specific functional properties [1]. It has been shown that curcumin (CU) as an active substance possesses significant anti-inflammatory, anti-oxidant, anti-carcinogenic, anti-mutagenic, anticoagulant, and anti-infective properties [7]. CU promotes healing by acting on various stages of the natural wound healing process. It can enhance granulation, tissue formation, collagen deposition, tissue remodelling, and wound contraction [7].

The aim of this study was to develop curcumin delivery systems made of degradable polymer microparticles and to assess their anti-inflammatory properties in contact with human macrophages.

## Materials and Methods

### Manufacturing of microparticles

Polymeric microparticles were manufactured using a single oil-in-water (O/W) emulsification with the solvent evaporation method. The water phase (W) was a 2% poly(vinyl alcohol) solution (PVA, Mw = 31 kDa, Sigma-Aldrich, Mowiol 4-88, CAS: 9002-89-5) while the oil phase (O) consisted of poly(sebacic anhydride) (PSA, Silesian University of Technology [10]) dissolved in dichloromethane (DCM, 99.8% pure P.A., POCH S.A, CAS: 75-09-2) (2% w/v) with CU (Sigma-Aldrich, C7727-500MG, CAS:458-37-7) as an active substance. The chemical formulas of CU and PSA are shown in FIG. 1 and 2, respectively.

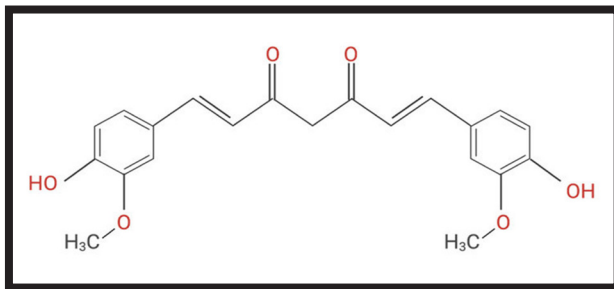


FIG. 1. Molecular structure of curcumin.

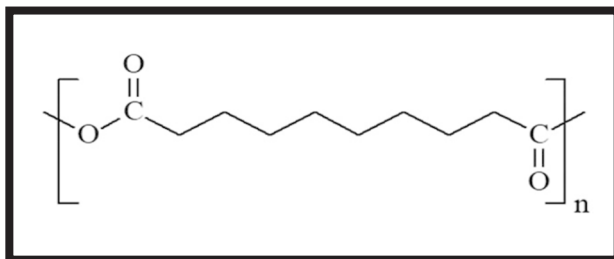


FIG. 2. Poly(sebacic anhydride) structural formula.

Polymeric microparticles that contained different weight concentrations of CU were prepared according to a method described earlier [11]: PSA/DCM – unloaded sample and PSA/DCM+CU with different concentrations of CU: 5, 10, and 20 wt% CU.

The calculated masses of curcumin required to prepare samples with CU concentrations: 0, 5, 10, and 20 wt%, were respectively weighted. Then, a 2% w/v PSA solution in DCM was prepared as an oil phase. 3 mL of the oil phase was homogenized for 90 s, at an amplitude of 40%, and slowly dripped into the water phase (20 mL). Subsequently, beakers placed in crystallizers with ice (to cool the PVA solution) were then placed on a magnetic stirrer to mix their contents.

The mixing process was carried out for 5 h (until the solvent evaporated), at a set stirring speed of 1200 rpm at room temperature. The resulting emulsions were then centrifuged using a centrifuge (3-30 K, Sigma). Centrifugation parameters were:  $v = 15,000$  rpm,  $t = 20$  min,  $T = 4^{\circ}\text{C}$ . Next, UHQ water was added and the samples were centrifuged 3 times. Supernatants (1.5 mL for each sample) were collected to assess encapsulation efficiency (EE). 10  $\mu\text{L}$  of the suspension was placed on a microscope slide and 3 images per sample were taken for further characterization of the manufactured microparticles. The remaining microparticles were frozen at  $-80^{\circ}\text{C}$  for 24 h. Microparticles were freeze-dried for 48 h.

The diameters of the manufactured polymeric microparticles were measured using ImageJ software. Histograms of the size distribution were prepared based on the obtained results using Python software.

Manufacturing efficiency (ME) was calculated using the formula (1):

$$\text{ME} = \frac{\text{mass of sample after lyophilization}}{\text{mass of PSA in sample} + \text{mass of CU in sample}} \cdot 100\% \quad (1)$$

### Characterization of microparticles

The encapsulation efficiency of CU was determined in the supernatants after the centrifugation process using a fluorometric assay. The supernatant samples were treated with DMSO (POCH S.A.) at a volume ratio of 1:10 to dilute the residual CU. CU in known concentrations (0-100  $\mu\text{g}/\text{mL}$ , step 10  $\mu\text{g}/\text{mL}$ ) was dissolved in the same mixture of water: DMSO (1:10) for the preparation of the calibration curve. The linear relationship was estimated in the range of 0-20  $\mu\text{g}/\text{mL}$  CU. Samples of both calibrators and supernatants diluted in DMSO were placed in a black 96-well TCPS plate (100  $\mu\text{L}/\text{well}$ ,  $n = 3$  for each sample). Excitation wavelengths of 485-412 nm and emission wavelengths of 590-510 nm were used in a plate reader (FluoStar OMEGA, BMG LabTech) [11].

The encapsulation efficiency (EE) was determined as (2):

$$\text{EE} = \frac{\text{encapsulated CU}}{\text{initial CU addition}} \cdot 100\% \quad (2)$$

and drug loading (DL) was calculated as follows (3):

$$\text{DL} = \frac{\text{encapsulated CU}}{\text{MP mass}} \cdot 100\% \quad (3)$$

FTIR analysis was performed using PerkinElmer FT-IR spectrometer to identify characteristic chemical groups and bonds present in the curcumin molecule, and to determine the encapsulation efficiency, a semi-quantification approach was used. The analysis was carried out at room temperature ( $21^{\circ}\text{C}$ ) and low humidity (approx. 68%). FTIR spectra were analyzed using PerkinElmer Spectrum IR software.

### Primary human monocyte isolation and macrophage differentiation

Human monocytes were isolated from the peripheral blood of healthy blood donors by negative selection, using methods described in [12]. Briefly, buffy coats were centrifuged at room temperature for 20 min at 1200 g (Eppendorf Centrifuge 5810R, VWR International LLC, Radnor, PA, USA), with acceleration set at 5 and brake set to 0, for blood components separation. Peripheral blood mononuclear cells (PBMC) were collected and incubated with RosetteSep™ Human Monocyte Enrichment Cocktail (67  $\mu\text{L}$  per 1 mL of RBC-PBMC, StemCell Technologies™, Vancouver, Canada) at room temperature for 20 min under slow orbital agitation. The mixture was diluted at a 1:1 ratio with 2% heat in-activated FBS (Biowest, Riverside, MO, USA) in PBS, gently layered over Histopaque-1077 (Sigma-Aldrich Co., St Louis, MO, USA) and centrifuged as former.

The enriched monocyte layer was collected and washed three times with PBS by centrifugation at 7 min, 1300 rpm, at room temperature (Eppendorf Centrifuge 5810R, VWR International LLC, Radnor, PA, USA) [13].

For macrophage differentiation,  $0.5 \times 10^6$  cells/mL were seeded on glass coverslips in 24-well plates, and cultured for 7 days in complete RPMI media, supplemented with 10% FBS, in the presence of 50 ng/mL of rh M-CSF (ImmunoTools, Friesoythe, Germany). After 7 days of differentiation, the cell culture media was changed, and M-CSF was removed [12,13].

To polarize macrophages towards M1 phenotype (pro-inflammatory), on day 7 of culture, media was replaced, and monocytes/macrophages were stimulated with 10 ng/mL lipopolysaccharide (LPS, *Escherichia coli* serotype O55:B5, Sigma-Aldrich Co., St Louis, MO, USA) and 50 ng/mL recombinant interferon-gamma (rhIFN- $\gamma$ , ImmunoTools, Friesoythe, Germany) [12].

The manufactured PSA-based microparticles were added to the activated cells on day 8 to investigate their anti-inflammatory properties, interpreted as the ability of the cells to shift their phenotype from M1 (pro-inflammatory) towards M2 (anti-inflammatory).

Evaluation of the cells morphology was performed by fluorescent staining with phalloidin red and DAPI. Briefly, cells were fixed with 4% paraformaldehyde solution (PFA: 50-00-0; Sigma-Aldrich®) for 20 min and afterward washed with PBS (3x5 min, under agitation). The aldehydes were blocked with ammonium chloride ( $\text{NH}_4\text{Cl}$ , 213330, Sigma-Aldrich®, 50 mM) for 10 min. Cells were washed with PBS (3x5 min). The membrane was permeabilized with 0.2% Triton X-100: 648466 (VWR International, Material de Laboratório, Lda) for 5 min. Cells were washed with PBS (3x5 min, under agitation), blocked with 1% bovine serum albumin (BSA: A4919, Sigma-Aldrich®), for 1 h, followed by an incubation with phalloidin red (1:200, Alexa Fluor™ 594 phalloidin: A12381, ThermoFisher Scientific, Invitrogen) for 20 min. Cells were washed with PBS (3x5 min, under agitation). Nuclei were stained with DAPI (1:1000, D3571; Alfacene) for 5 min. PBS washing was repeated (3x5 min, under agitation). All steps were performed at room temperature (RT, 21°C). Images were taken under a motorized inverted epifluorescence microscope (Leica DMI6000 FFW, Leica Microsystems, Germany).

LDH assay (Promega) was performed to assess the cytotoxicity of the developed particles. The assay was conducted on the following types of samples: CU, unloaded microparticles (PSA-based), and microparticle samples with CU at the concentrations of 0.77 mg/mL, and 1.54 mg/mL. Briefly, a 50  $\mu\text{L}$  medium of each sample was placed in the wells of a 96-well plate. Next, 50  $\mu\text{L}$  of CytoTox96® Assay (Promega, Madison, WI, USA), was added to bind with LDH, and the plate was left to incubate for 30 min (protected from light). Next, 50  $\mu\text{L}$  of stop solution was added to block the reaction. A blank control (only a culture medium) and a positive control were also included. Cytotoxicity was defined as the percentage of LDH activity in culture media, relative to LDH activity of the positive control [13]. The presence of LDH was measured in cell-free culture supernatants. The total LDH release was determined using LDH positive control provided by the CytoTox96® assay. Three replicates for each measurement were included for each condition. The average of the three measurements was determined.

24 hours after incubation of macrophages with microparticles, macrophage polarization was evaluated by flow cytometry. Macrophages were identified using the following surface markers: CD14 (as a pan macrophage marker), CD86 (M1 phenotype), and CD163 (M2 phenotype). 2  $\mu\text{L}$  for CD14 and CD86 marker, and 5  $\mu\text{L}$  for CD163 marker was added to the corresponding well.

The following samples were analyzed: control sample (primary human macrophages), CU powder, unloaded microparticles (PSA-based matrix, MPs), and polymeric microparticles loaded with curcumin at a concentration of 0.77 mg/mL (MPs\_CU\_0.77) and 1.54 mg/mL (MPs\_CU\_1.54).

The macrophages were washed, resuspended in FACS buffer (PBS, 2% FBS, 0.01% sodium azide) (Sigma-Aldrich Co., St Louis, MO, USA) and incubated with the following antibodies: anti-human CD14-APC (clone MEM-18), CD86-FITC (clone BU63) (all from ImmunoTools, Friesoythe, Germany) and CD163-PE (clone GHI/61) (BD Biosciences, San Jose, CA, USA) for 30 min at RT. Isotype-matched antibodies were used as negative controls, to define background staining [12].

After additional washing, 10,000 cells, gated according to forward and side scatter parameters, were acquired using a BD FACSCanto IITM flow cytometer (Becton Dickinson) using FACSDiva™ software (both from BD Biosciences, San Jose, CA, USA). Data were analyzed using FlowJo software (BD Biosciences, San Jose, CA, USA, version 10), and the percentage of CD14, CD86, and CD163 positive cells was calculated by subtracting the corresponding isotype control [12].

## Results and Discussion

### Properties of microparticles

The preparation method of microparticles was emulsification with solvent evaporation. The following sample types were analyzed: pure CU powder, unloaded PSA microparticles, and curcumin-loaded microparticles with concentrations of 5, 10, and 20% by weight of CU. The highest manufacturing efficiency was obtained for a polymeric sample with a concentration of 10 wt% CU, and it was equal to 74%. The manufactured PSA-based microparticles were spherical with a median diameter from 5.2 to 8.4  $\mu\text{m}$  (FIG. 3A-H). The CU-loaded microparticles were yellow (FIG. 4B-D) and because of the fact that CU is fluorescent, the microparticles glowed intensely green under the fluorescence microscope, and exhibited fluorescent properties (FIG. 4B-D). It indicated that CU was effectively and uniformly encapsulated within the PSA microparticles (only black background was visible in CU-free sample image, FIG. 4A). The fluorescence of curcumin allowed the encapsulation and loading efficiency to be tested with a fluorescence reader, so the fluorescence images obtained (FIG. 4) not only prove the presence of curcumin in the particles, but also confirm the fact that it is fluorescent and explain the basis for the choice of this particular research method.

### Encapsulation efficiency and loading efficiency

Encapsulation efficiency (EE) of CU in microparticles was calculated using a calibration curve, separately for supernatants and particles alone (TABLE 1). Supernatant analysis may not provide accurate results of encapsulation efficiency, hence, an analogous analysis was carried out with a calibration curve to determine encapsulation efficiency involving microparticles alone. The highest EE was observed for a concentration of 5 and 10 wt% CU. For 20 wt% CU EE was significantly lower presumably due to the oversaturation phenomenon. The calculated values of drug loading reached values very close to those assumed. The slight differences observed are due to unavoidable curcumin and polymer losses at the manufacturing stage.

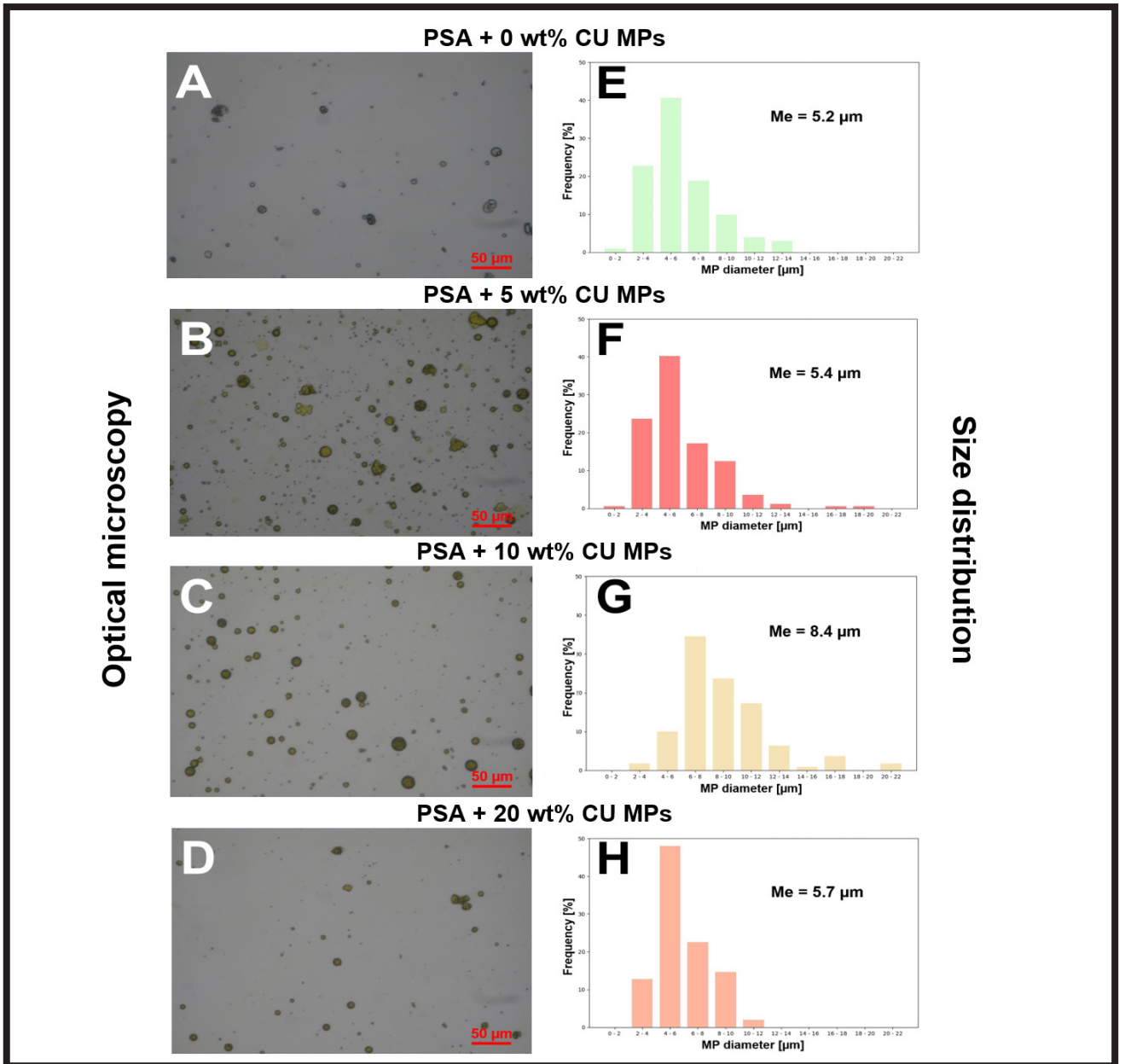


FIG. 3. Morphology (A, B, C, D) and size distribution (E, F, G, H) of PSA microparticles with different concentrations: 0 wt% CU – unloaded (A, E), 5 wt% CU (B, F), 10 wt% CU (C, G), and 20 wt% CU (D, H).

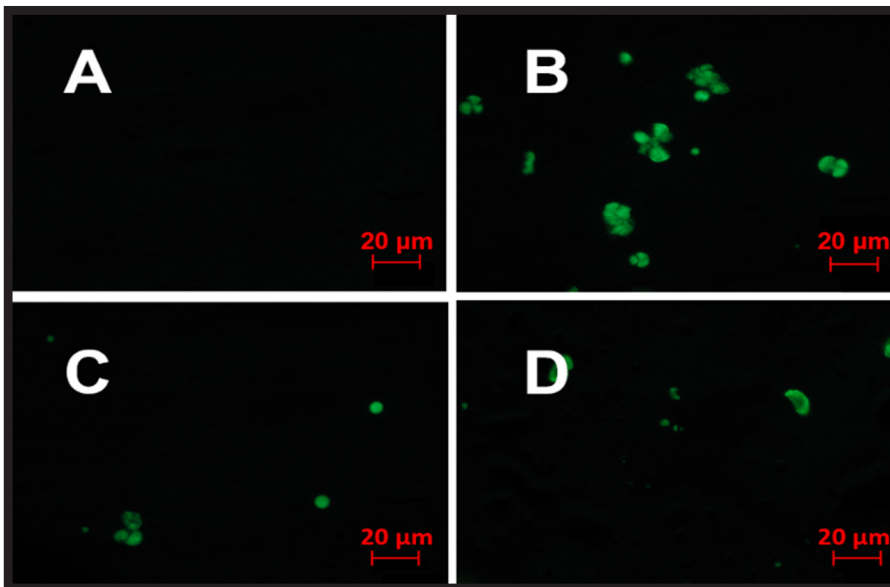


FIG. 4. Pictures from the fluorescent microscope of MPs obtained with CU: PSA with different concentrations of CU: 0 wt% CU – unloaded (A), 5 wt% CU (B), 10 wt% CU (C), 20 wt% CU (D).

**TABLE 1. Curcumin encapsulation efficiency and loading in PSA+CU microparticles.**

Curcumin concentration (Expected) [%]	Encapsulation efficiency EE [%]		Loading efficiency DL [%]
	supernatant analysis	microparticle analysis	
5	81.70	72.00	5.39
10	79.50	72.50	10.53
20	58.00	52.70	17.60

### FTIR analysis

The presence of CU was also determined by a semi-quantitative analysis using FTIR. FTIR analysis was performed to identify characteristic functional groups and bonds present in the curcumin molecule, confirming their successful encapsulation in the polymer carrier. Curcumin shows a characteristic band at  $1510\text{ cm}^{-1}$ , which originates from the stretching vibrations of the C=C bonds of the aromatic ring (FIG. 5A). The spectra of the analyzed polymeric microparticle samples with encapsulated CU also show the presence of this characteristic peak at  $1510\text{ cm}^{-1}$  (FIG. 5C-E), indicating effective encapsulation of CU in the PSA-based matrix. The intensity of this peak is highest for CU powder. For PSA samples with encapsulated CU (concentrations of 5, 10, and 20 wt% CU), the intensity of the peak changes in the same way as the encapsulation efficiency.

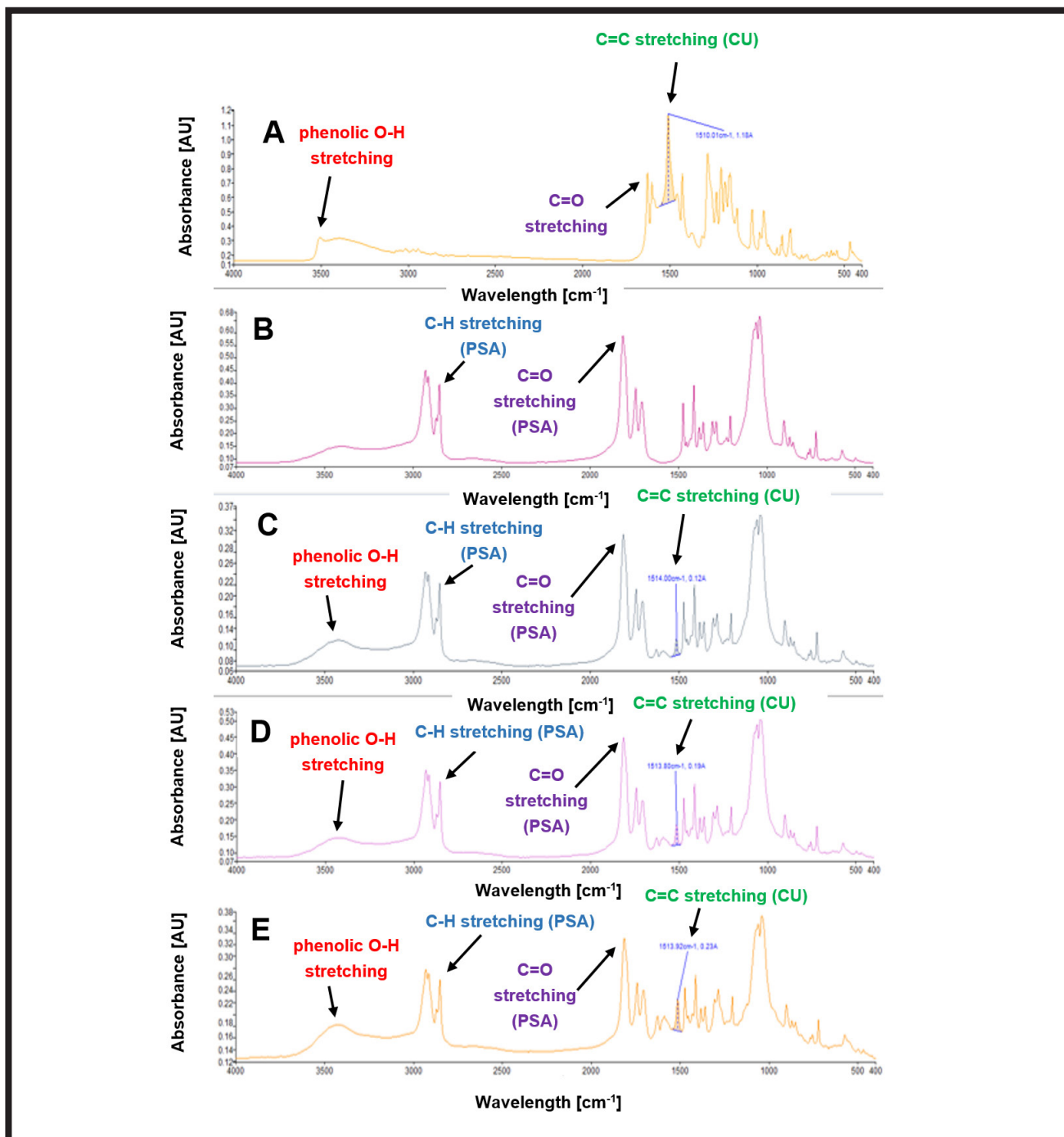


**FIG. 5. FTIR spectra of the analyzed samples: CU powder (A), unloaded microparticles (B), and microparticles loaded with 5 wt% CU (C), 10 wt% CU (D), and 20 wt% CU (E).**

It increases as the weight concentration of CU increases, with the peak intensity decreasing once the supersaturation value (20 wt% CU) is reached. For the unloaded microparticles sample (FIG. 5B) no peak is observed at this wavelength, indicating that CU is not present in this sample. In addition, the band from phenolic O-H stretching is present in the CU molecule (FIG. 5A) and CU-loaded samples (FIG. 5C-E) and it is absent in the PSA molecule (FIG. 5B). The characteristic functional groups for the PSA molecule (C=O carbonyl group) present at 1816  $\text{cm}^{-1}$  and 2800  $\text{cm}^{-1}$  (C-H stretching vibrations) were also identified and analyzed (FIG. 5B-E).

A semi-quantitative determination was carried out by analyzing the area under the curve (AUC) formed by the respective bands corresponding to the characteristic functional groups of CU and PSA. Ratios of AUC of the characteristic CU to PSA (1816  $\text{cm}^{-1}$  to 1510  $\text{cm}^{-1}$ ) peaks may correspond to the encapsulation efficiency of CU. The ratio of PSA to PSA peaks may be an indication of the possible CU and PSA interactions. The ratio of AUC of two characteristic peaks for PSA (i.e. at 1816  $\text{cm}^{-1}$  and 2800  $\text{cm}^{-1}$ ) was similar for all the CU-encapsulated samples, and it was higher than that for unloaded PSA microparticles; it may suggest the formation of CU-PSA bonds, probably hydrogen bonds. The ratio of AUC for the characteristic bands for CU and PSA increased for all microparticles containing CU as compared to pure CU powder. It might be proof that encapsulation was effective, but there was no direct correlation between this ratio and the expected CU loading.

#### **In vitro studies with primary human macrophages**

24 hours after macrophage activation towards M1 phenotype, microparticles of defined concentrations, together with a sample of CU powder, were dissolved in the culture medium. As a control sample, primary human macrophages alone were used. The following suspension samples of microparticles in RPMI media (concentration of CU in cell media) were tested: pure CU powder (CU at a concentration equal to 16.7 mg/mL), unloaded PSA microparticles (MPs at a concentration equal to 7.3 mg/mL), microparticles loaded with CU and tested at the concentration of 0.77 mg/mL (MPs\_CU\_0.77) and the concentration of 1.54 mg/mL (MPs\_CU\_1.54).

#### **LDH assay**

The LDH assay was performed on primary human macrophages. Cell death was assessed by the CytoTox96<sup>®</sup> assay which measures the activity of LDH released from apoptotic cells. Total LDH release was determined using LDH positive control. Cytotoxicity was defined as the percentage of LDH activity in the culture supernatants, relative to LDH activity of the positive control. The positive control was all living cells and the negative control was all dead cells. The level of control 100% (the ratio of positive to negative controls, multiplied by 100%) is equal to 54.22%. Control 100% refers to cell death. Above the line, an analyzed sample is considered cytotoxic. Three replicates for each measurement were included for each condition. The average of the three measurements was then determined. The percentage of LDH released into the culture medium was calculated as the ratio of the average to the negative control, multiplied by 100%. Based on the results, column graphs were prepared to show the % of LDH release (cell viability) for the analyzed concentrations (FIG. 6). The 100% control level was also highlighted, which marks the threshold above which the analyzed samples show a cytotoxic effect on primary human macrophages.

The results of LDH assay (FIG. 6) showed no cytotoxicity of the tested samples when cultured with primary human macrophages.

#### **Fluorescent staining with phalloidin red and DAPI**

Cell morphology was characterized using fluorescence microscopy images (Leica DMI6000 FFW, Leica Microsystems, Germany). The images were obtained at x20 magnification (FIG. 7). It was observed that when microparticles (both unloaded and curcumin-loaded) and pure CU powder were added, the cell morphology did not change. The cultured cells in contact with the added microparticles were randomly dispersed, forming numerous cell agglomerates.

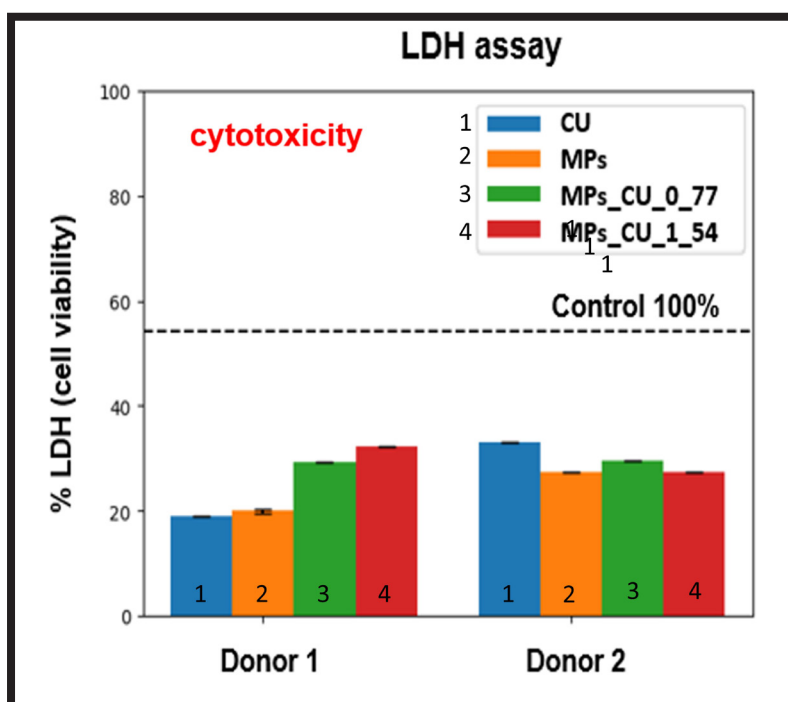
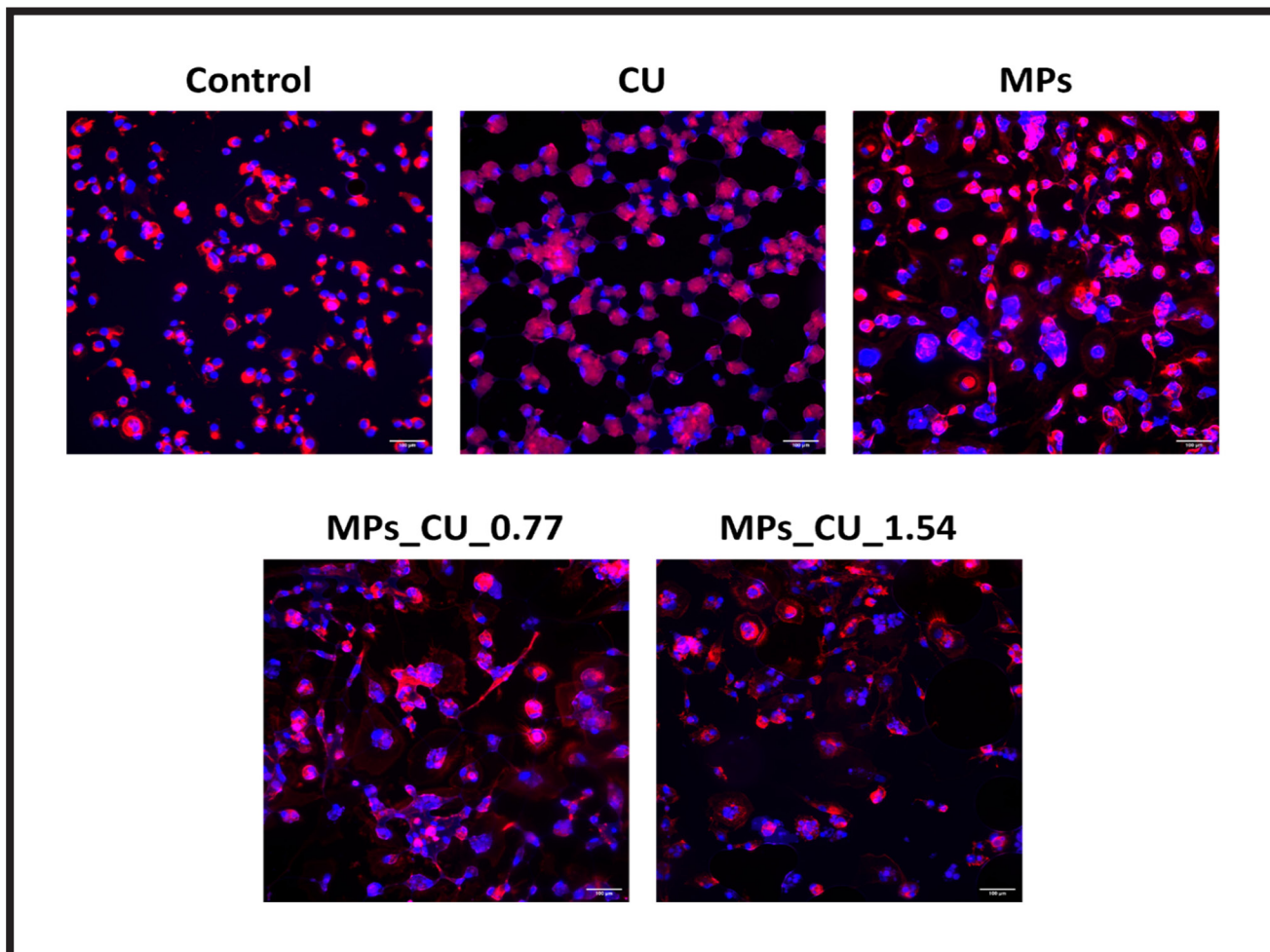


FIG. 6. Cytotoxicity assessed by the LDH assay in primary human macrophages, in contact with pure CU powder (CU), unloaded PSA microparticles (MPs), microparticles loaded with CU and tested at concentration 0.77 mg/mL (MPs\_CU\_0.77) and at concentration 1.54 mg/mL (MPs\_CU\_1.54). The 100% control represents the ratio between negative and positive controls, multiplied by 100%. n = 2.



**FIG. 7.** Fluorescence microscopy images, at x20 objective, of human primary macrophages, derived from Donor 1, cultured in contact, for 24 h, with the following samples: control (cell culture medium), CU (curcumin powder), MPs – unloaded microparticles (PSA), and microparticles loaded with CU and tested at concentration of 0.77 mg/mL (MPs\_CU\_0.77) and at concentration of 1.54 mg/mL (MPs\_CU\_1.54).

### Flow cytometry

After 24 h, the macrophages cultured with the prepared microparticles samples were collected and analyzed by flow cytometry. Dot plots from a representative experiment are presented in FIG. 8. Within each representative dot plot, a corresponding gate was determined that plotted the range of cells analyzed (TABLE 2). Gate selection (FIG. 8a-e) determines the entire cell population, which is then analyzed and assigned to phenotype M0, M1, or M2 (TABLE 2), depending on the quadrant in which the cell is located (FIG. 8A-E).

The M2/M1 ratio (number of macrophages with anti-inflammatory phenotype/number of macrophages with pro-inflammatory phenotype) is an important parameter in the context of evaluating anti-inflammatory properties. The flow cytometry analysis of macrophages was carried out for two different human donors. The results of calculating the average M2/M1 phenotypic ratio for the two donors studied (the microparticle samples analyzed were CU, MPs, MPs\_CU\_0.77, and MPs\_CU\_1.54) are shown in TABLE 2. The results obtained indicate that the presence of CU increases the M2/M1 phenotypic ratio, promoting macrophage polarization towards the M2 (anti-inflammatory) phenotype.

Based on the data collected in TABLE 2, the values of the M2/M1 phenotypic ratios for the two different donors are presented graphically in FIG. 9 as Average  $\pm$  standard deviation of the sample (SD). The results show that the addition of CU or CU-loaded microparticles to the cell culture media results in an increased M2/M1 ratio.

The M2/M1 ratio for the samples with CU and CU powder is significantly higher than for the samples unloaded with CU. At the same time, the flow cytometry results indicated the presence of only a few anti-inflammatory cells, which may suggest that PSA-based microparticles with encapsulated curcumin at the concentrations tested in this research do not exhibit sufficient anti-inflammatory properties to reduce inflammation at the wound site. Therefore, it would be interesting for future studies to test earlier time points (for example, less than 24 h). To obtain more reliable results, it would be necessary to increase the number of donors.

### Ethics statement

Human primary monocytes were isolated from surplus buffy coats from healthy blood donors, kindly donated by Serviço de Imunohemoterapia, Centro Hospitalar Universitário de São João (CHUSJ), Porto. All obtained human samples and procedures were performed in agreement with the principles of the Declaration of Helsinki and all experimental protocols were conducted following the approval and recommendations of the CHUSJ Ethics Committee for Health (references 90/19 and 260/11). Written informed consent was obtained from all subjects before sample collection. Buffy coat samples were provided anonymized and patient identification was not provided to researchers.

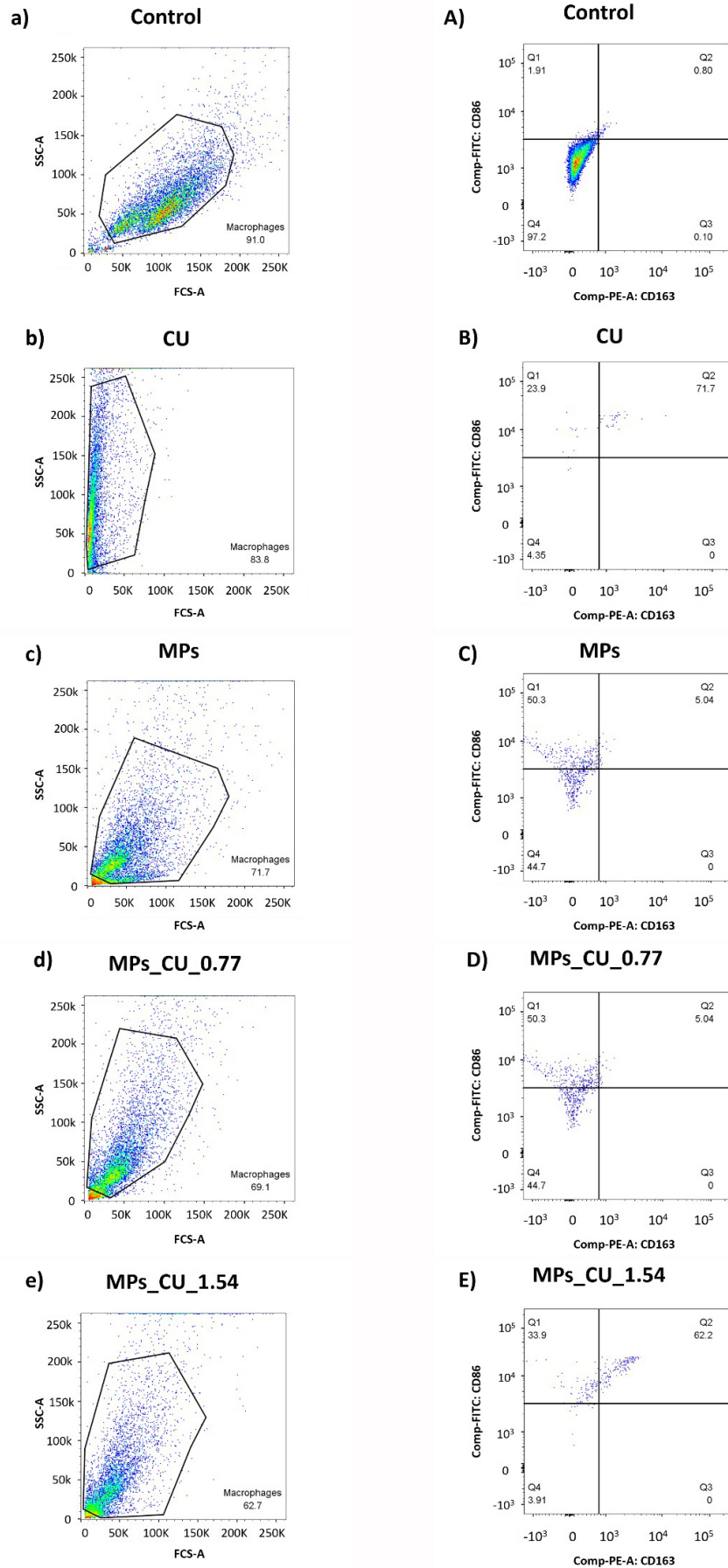


**FIG. 8.** Expression of cell surface markers on macrophages. Representative dot plots showing: a)-e) aspect ratio; A)-E) expression of CD14, CD86, and CD163 antigens. Gates were drawn from isotype control staining. Percentage of CD14 positive cells expressing CD163 (M2 marker) and/or CD86 (M1 marker) antigens (FSC: forward scatter; SSC: side scatter).

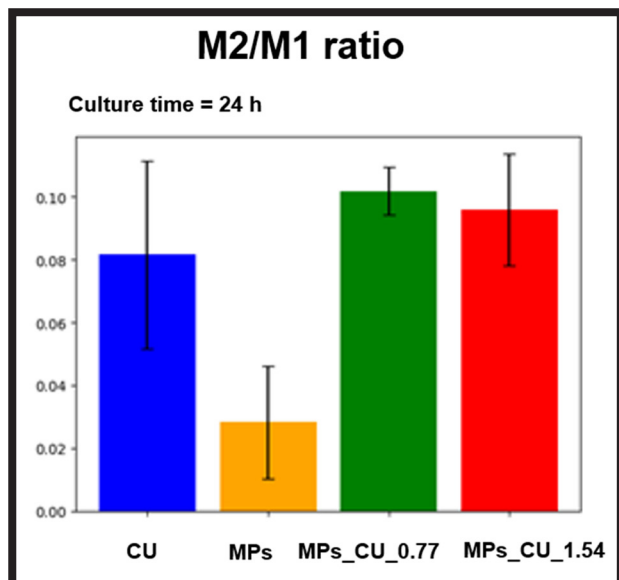


FIG. 9. Characterization of the averaged ratio M2 to M1 macrophages from two donors as studied by flow cytometry in contact with the following samples: CU, MPs, MPs\_CU\_0.77, and MPs\_CU\_1.54.

## Conclusions

In this study, PSA microparticles loaded with CU were developed as a component of dressing for the treatment of ulcers occurring in diabetic foot syndrome. The carriers were spherical and of the 5-8  $\mu\text{m}$  median size, thus suitable to be suspended in topical formulations administered to wounded skin [14]. Encapsulation efficiency of 72% was achieved for the sample with 10 wt% CU microparticles. The presence of CU in microparticles was also confirmed by:

- 1) visual inspection (yellow colour contrarily to white colour for unloaded microparticles, FIG. 3);
- 2) fluorescent properties (polymer matrix does not exhibit fluorescence but curcumin molecule does, FIG. 4);
- 3) presence of bands in FTIR spectra characteristic for pure curcumin (FIG. 5).

CU carriers were tested for cytotoxicity in contact with primary human macrophages. Their phenotype (M1-pro-inflammatory, M2-anti-inflammatory) and M2/M1 ratio were determined by flow cytometry analysis. The LDH tests showed that the obtained microparticles are not cytotoxic and that the phenotypic M2/M1 ratio for samples with CU and CU powder is higher than for samples without CU. This confirms that curcumin released from the microparticles is able to increase the polarization of macrophages toward an anti-inflammatory phenotype, what may be explored in the development of dressings for the treatment of diabetic foot ulcers.

TABLE 2. Flow cytometry analysis of studied macrophages (number of cells) from two different donors shown as average and SD.

Sample	CD14	CD86 (M1)	CD163 (M2)	Ratio M2/M1 Average $\pm$ SD
CU	1659	17355	1424	0.082 $\pm$ 0.029
MPs	2017	4081	114	0.028 $\pm$ 0.082
MPs_CU_0.77	1955	10451	1064	0.102 $\pm$ 0.007
MPs_CU_1.54	1662	13106	1256	0.096 $\pm$ 0.018

Culture time = 24 h

## Acknowledgements

The research was supported by the subsidy (No 16.16.160.557) for the AGH University of Krakow, and the Norte Regional Operational Program, Portugal – Structured R&D&I Projects – Unorte.pt. HEALTH-UNORTE; NORTE-01-0145-FEDER 000039 for i3s Institute, Porto. KW is acknowledging Erasmus Plus program for the support of her stay at i3S – Instituto de Investigação e Inovação em Saúde, Universidade do Porto. The authors thank Prof. Katarzyna Jaszcz from Silesia University of Technology for providing poly(sebacic anhydride) samples.

## ORCID iD

- K. Wójcik: <https://orcid.org/0009-0005-0944-0234>  
 A. Kusibab: <https://orcid.org/0000-0002-5580-7392>  
 A.B. Sousa: <https://orcid.org/0000-0002-3460-0499>  
 J. Novais Barbosa: <https://orcid.org/0000-0003-1852-2790>  
 E. Pamuła: <https://orcid.org/0000-0002-0464-6189>

## References

- [1] Kandregula B., Narisepalli S., Chitkara D.: Exploration of Lipid-Based Nanocarriers as Drug Delivery Systems in Diabetic Foot Ulcer. *Molecular Pharmaceutics* 19(7) (2022) 1977–1998, doi:10.1021/acs.molpharmaceut.1c00970.
- [2] Gowthamarajan K., Karri V.V.S.R., Satish Kumar M.N.: Multiple Biological Actions of Curcumin in the Management of Diabetic Foot Ulcer Complications: A Systematic Review. *Tropical Medicine and Surgery* 3 (2015) 179, doi:10.4172/2329-9088.1000179.
- [3] Akhtar S., Latif M., Ahmed O.S., Sarwar A., Alina A., Khan M.I.: Prevalence of foot ulcers in diabetic patients in Punjab, Pakistan. *Frontiers in Public Health* 8(10) (2022) 967733, doi:10.3389/fpubh.2022.967733.
- [4] Salad A.M., Duale H.A., Sheikh I.M., Hassan G.D., Farah A.A., Gele A.: Prevalence of diabetes foot ulcers and associated factors among adult diabetic patients in three referral hospitals in Mogadishu, Somalia. *Frontiers in Public Health* 11 (2023) 1195483, doi:10.3389/fpubh.2023.1195483.
- [5] Driver V.R., Fabbi M., Lavery L.A., Gibbons G.: The costs of diabetic foot: The economic case for the limb salvage team. *Journal of Vascular Surgery* 52(3) (2010) 17S-22S, doi:10.1016/j.jvs.2010.06.003.
- [6] Spampinato S.F., Caruso G.I., De Pasquale R., Sortino M.A., Merlo S.: The Treatment of Impaired Wound Healing in Diabetes: Looking among Old Drugs. *Pharmaceutics* 13(4) (2020) 60, doi:10.3390/ph13040060.
- [7] Akbik D., Ghadiri M., Chrzanowski W., Rohanizadeh R.: Curcumin as a wound healing agent. *Life Sciences* 116(1) (2014) 1–7, doi:10.1016/j.lfs.2014.08.016.
- [8] Krzyszczuk P., Schloss R., Palmer A., Berthiaume F.: The Role of Macrophages in Acute and Chronic Wound Healing and Interventions to Promote Pro-wound Healing Phenotypes. *Frontiers in Physiology* 9 (2018) 419, doi:10.3389/fphys.2018.00419.
- [9] Sousa A.B., Águas A.P., Barbosa M.A., Barbosa J.N.: Immunomodulatory biomaterial-based wound dressings advance the healing of chronic wounds via regulating macrophage behaviour. *Regenerative Biomaterials* 9 (2022) rbac065, doi:10.1093/rb/rbac065.
- [10] Jaszcz K.: Synthesis and Characterization of New Functional Poly(ester-anhydride)s Based on Succinic and Sebacic Acids. *Macromolecular Symposia* 254(1) (2007) 109–116, doi:10.1002/masy.200750817.
- [11] Kwiecień K., Reczyńska-Kolman K., Niewolik D., Jaszcz K., Pamuła E.: Poly(sebacic anhydride) microparticles loaded with curcumin for pulmonary purposes. *Engineering of Biomaterials* 162(24) (2021), doi:10.34821/eng.biomat.162.2021.7-12.
- [12] Oliveira M.I., Pinto M.L., Gonçalves R.M., Martins M.C.L., Santos S.G., Barbosa M.A.: Adsorbed Fibrinogen stimulates TLR-4 on monocytes and induces BMP-2 expression. *Acta Biomaterialia* 49 (2017) 296–305, doi:10.1016/j.actbio.2016.11.034.
- [13] Bessa-Gonçalves M., Silva A.M., Brás J.P., Helmholz H., Luthringer-Feyerabend B.J.C., Willumeit-Römer R., Barbosa M.A., Santos S.G.: Fibrinogen and magnesium combination biomaterials modulate macrophage phenotype, NF-κB signaling and crosstalk with mesenchymal stem/stromal cells. *Acta Biomaterialia* 114 (2020) 471–484, doi:10.1016/j.actbio.2020.07.028.
- [14] Reczyńska-Kolman K., Hartman K., Kwiecień K., Brzychczy-Włoch M., Pamuła E.: Composites Based on Gellan Gum, Alginate and Nisin-Enriched Lipid Nanoparticles for the Treatment of Infected Wounds. *International Journal of Molecular Sciences* 23(1) (2022) 321, doi:10.3390/ijms23010321.

# CHARACTERISTIC OF FISH COLLAGEN FILMS CROSS-LINKED WITH GLUTARALDEHYDE

KAROLINA KULKA-KAMIŃSKA<sup>1\*</sup> ,  
PATRYCJA BRUDZYŃSKA<sup>1</sup> , ALINA SIONKOWSKA<sup>1</sup> ,  
KATARZYNA LEWANDOWSKA<sup>1</sup> , ŁUKASZ PIWOWARSKI<sup>2</sup> 

<sup>1</sup> DEPARTMENT OF CHEMISTRY OF BIOMATERIALS AND COSMETICS, NICOLAUS COPERNICUS UNIVERSITY IN TORUŃ, UL. GAGARINA 7, 87-100 TORUŃ, POLAND

<sup>2</sup> SANCOLL SP. Z O.O., UL. JULIUSZA SŁOWACKIEGO 24, 35-060 RZESZÓW, POLAND

\*E-MAIL: KKULKA@DOKTORANT.UMK.PL

## Abstract

Collagen is a valuable biopolymer in many fields, especially in biomedical sciences. Thanks to its biodegradability and high biocompatibility, it is a desirable material for applications that require contact with the human body. There are many sources of collagen, of which marine-origin collagen has become an important one in recent times. Pure collagen has poor stability and is sensitive to the effects of heat and other external factors. The cross-linking process can improve the properties of collagen materials. Many different methods of cross-linking can be distinguished, including chemical ones. In this study, we were concerned to obtain collagen films modified with glutaraldehyde (GTA). The influence of this additive on the chemical, mechanical, swelling, and hydrophilic properties of the biopolymeric matrix was evaluated. Two different concentrations of collagen were used, as well as three different concentrations of GTA. Results of the analysis showed that the properties of the obtained films were affected by the addition of even a small amount of cross-linker. Spectroscopic measurements indicated minor changes that reflect interactions between GTA and the collagen matrix. Mechanical tests showed changes for modified samples in values of tensile strength, breaking force, and elongation at break. The hydrophilicity decreased slightly for films with GTA. The durability of the modified samples in the swelling test increased. Differences between 1% and 2% collagen films with additives were also observed. The GTA-obtained fish collagen films can be promising materials for biomedical applications.

**Keywords:** collagen, glutaraldehyde, cross-linking, polymer films, marine sources

[Engineering of Biomaterials 168 (2023) 25-32]

doi:10.34821/eng.biomat.168.2023.25-32

Submitted: 2023-05-05, Accepted: 2023-05-19, Published: 2023-05-25



Copyright © 2023 by the authors. Some rights reserved.  
Except otherwise noted, this work is licensed under  
<https://creativecommons.org/licenses/by/4.0>

## Introduction

Collagen is a relevant biopolymer that occurs in living organisms. This fibrous protein constitutes 30% of vertebrates' bodies and supports the structural integrity and functions of tissues [1], and helps maintain mechanical and structural functions in organisms [2]. This polypeptide builds human skin, tendons, cartilage, bone tissue, and blood vessels [3,4].

There are 29 types of collagen that are genetically different. They differ in the sequence of the primary amino acids in their polypeptide chains [4]. Types I, II, and III are the main types of collagen in humans [5]. Type I mainly builds the skin and represents 80-95% of skin collagen; it is a crucial component of the extracellular matrix (ECM). Type II is predominantly found in cartilage, while type III is often found along with type I and usually makes up approximately 15% of skin collagen [6,7]. The helical structure, also known as the triple helix domain (COL), is the most characteristic feature of all types of collagen [8]. Collagens are highly organized supramolecular structures composed of three polypeptide chains with the characteristic amino acid sequence Gly-X-Y (Gly – glycine, X and Y usually represent proline, lysine, hydroxyproline, and hydroxylysine) which create tropocollagen. Tropocollagen molecules aggregate in fibrils that are subsequently cross-linked (maturation process) and finally create collagen fibrils [7,8]. Collagen biosynthesis involves a few steps: triple helix formation and post-translational modifications - enzymatic glycosylation, lysine hydroxylation, proteolytic cleavage of procollagen and formation of intra- and intermolecular cross-links [8]. Collagen triple helix is unique among other biopolymers due to the hydrogen bonds distribution that occurs only between polypeptide chains; there are no direct intramolecular hydrogen bonds [8].

Collagen as a biopolymer is a biocompatible, bioactive, and biodegradable material useful in biomedical applications. It is the best known protein-based material for skin scaffolds and wound dressings [9]. It can also be used in drug delivery systems, injectable dispersions, scaffolds for bone regeneration, cardiology, ophthalmology, and urology treatments [10]. The collagen used in these applications is of animal origin. Bovine collagen from skin and bone is of major industrial importance [10]. Another important source is the pig skin and bones. This collagen is very similar to human collagen, so it is much safer than the bovine in terms of allergenic potential [11], however, it is important to look for alternative sources due to the risk of zoonotic diseases [10]. Both bovine and porcine collagen carry the risks of contamination and, in addition, in the case of porcine collagen, religious issues remain a problem. In contrast to the collagen used in the industry, collagen obtained from rat tails is of great importance among the collagens used by scientists [9]. The search for new sources of collagen other than mammalian collagen is becoming more and more common [5]. A popular and convenient solution is marine-origin collagen, in particular from fish, derived from waste, which is safer and constitutes a part of the zero-waste trend. There are many advantages of marine sources, for example, high collagen content, environmental friendliness, low biological contamination and toxins content, minor regulatory problems, and low immunogenicity [10,12]. In addition to fish, other sources of collagen include jellyfish, sponges, starfish, octopus, and prawn [10,13]. For this purpose, almost all parts of the fish are used, including skin, bones, fins, and scales [9,10].

The fish that are often used for collagen extraction are as follows: cod *Gadus morhua*, white carp *Hypophthalmichthys molitrix*, yellowfish tuna *Thunnus albacares*, swordfish *Xiphias gladius*, tilapia *Oreochromis niloticus*, carp *Cyprinus carpio*, grouper *Epinephelus marginatus*, monkfish *Lophius piscatorius* [10,14-16]. Fish collagen contains less hydroxyproline in the polypeptide chain than mammalian collagen, which influences the denaturation temperature, which is much lower than in mammalian collagen. However, compared to collagen from other species of fish, collagen from silver carp is more resistant to high temperatures [17]. Slightly different characteristics, including denaturation temperatures, may occur in different species of marine organisms [16].

In terms of improving the physicochemical properties of collagen, some treatments can be performed, for example, the cross-linking process. Pure collagen is a structure that requires stabilization due to its poor resistance to high temperatures and other external factors [3]. Chemical and physical methods of cross-linking can be distinguished. Stabilization of the collagen structure can be achieved by the formation of new bonds, in the case of chemical cross-linking, functional groups are involved in this process [3]. Cross-linking is useful in the production of collagen scaffolds with properties similar to those of human tissues and organs [18]. The most commonly used chemical cross-linking agents are glutaraldehyde (GTA), dialdehyde starch (DAS), genipin, and EDC-NHS [3,18,19].

Glutaraldehyde (GTA) as a cross-linker provides enzymatic and thermal stability, as well as mechanical strength of the collagen biomaterial [18]. This chemical compound added to collagen generates a stiff network and causes the creation of covalent bonds between polypeptide chains [3]. Unfortunately, as a result of the toxicity of this substance, it cannot be used in all types of applications. It is important to use the appropriate concentration of GTA to maintain the balance between the desirable physicochemical properties of collagen-based material and low toxicity [18].

Researchers used different concentrations of glutaraldehyde as a cross-linking additive and different methods of treatment. Peng et al. prepared collagen sponges stabilized by GTA using the vapour cross-linking method [20]. They prepared more than 20 ml of glutaraldehyde solutions at different concentrations (5%, 10%, 15%, 20%, 25%) and placed in the lower part of the desiccators. The samples were exposed to GTA for up to 48 h. The results showed that complete cross-linking can be obtained with GTA concentrations of 20% and 25%, at lower concentrations cross-linking is not observed for this method [20]. In other research with dermal sheep collagen (DSC), scientists used 0.5% (w/w) of GTA solution to rinse the samples for 30 min. The results showed that this cross-linking compound can be very effective in the stabilizing of collagen-based materials [21]. The cross-linking mechanism of GTA is still under investigation. However, lysine or hydroxylysine is involved in the formation of cross-links with GTA [3].

In this study, we investigated the effect of the addition of glutaraldehyde (GTA) on the properties of fish collagen films. The films were obtained by the solvent casting method. To characterize the biopolymer films, a series of tests were carried out. Infrared spectroscopic analysis, mechanical test, swelling and degradation analysis, as well as contact angle measurements, were performed. The influence of different concentrations of GTA as an additive as well as two concentrations of collagen on the properties of the film was evaluated.

## Materials and Methods

### Preparation of biopolymer solution and films

1% and 2% (w/w) collagen solutions were prepared by dissolving freeze-dried collagen sheets from skins of silver carp fish (obtained by SanColl Sp. z o.o., Poland) in 0.1M acetic acid (Stanlab; Lublin, Poland). The obtained solutions were shaken and then stirred on a magnetic stirrer. The complete dissolution process took several days.

Collagen films were obtained following the solution casting method. Pure collagen films were prepared by pouring 30 g of solution onto a polystyrene plate (10 cm x 10 cm). GTA solution was prepared (12 mg/mL). To obtain the films, 1 ml, 2 ml and 5 ml of glutaric dialdehyde (GTA; Acros Organic; Geel, Belgium) were added to the weighted initial collagen solutions, respectively. The modified solutions were stirred on a magnetic stirrer for 5 min and then poured onto polystyrene plates and allowed to dry.

### FTIR spectroscopy

Infrared spectra were recorded using Nicolet iS10 equipment with a diamond ATR prism crystal accessory (Thermo Fisher Scientific, Waltham, MA, USA). Measurements were conducted with a resolution of 4 cm<sup>-1</sup>, in the wavenumber range of 400-4000 cm<sup>-1</sup>, and using 64 scans.

### Mechanical analysis

The mechanical properties of the samples were examined using a mechanical testing machine (Z.05, Zwick and Roell, Ulm, Germany). The following parameters were determined: Young's modulus (GPa), tensile strength (MPa), breaking force (N), and elongation at break (%). The speed starting position was 50 mm/min, the speed of the initial force was 5 mm/min, and the initial force was 0.1 MPa. The TestXpert II 2017 program was used to collect the data, the results were presented as average values and standard deviation. The average thickness of the collagen films was approximately 0.02 and 0.03 mm for 1% and 2% collagen, respectively.

### Swelling and degradation test

Collagen films were cut into squares of weight about 0.0050 g. Each type of sample (five squares in one series) was placed in a container with 50 ml of phosphate buffer saline (PBS). The weight measurements of the samples were conducted after 1 h, 2 h, 4 h, 8 h, 24 h, 48 h, 72 h, 1 week, and 2 weeks. The swelling degrees were calculated using the equation:

$$\text{swelling} = \frac{(m_t - m_0)}{m_0} \cdot 100\% \quad [\%]$$

$m_t$  – weight of the material after immersion in PBS [g]  
 $m_0$  – the initial weight of the material [g]

### Contact angle

Contact angle measurements of two liquids (glycerine (G) and diiodomethane (D)) were performed using a goniometer equipped with drop shape analysis (DSA 10 produced by Krüss, Germany). All measurements were carried out at room temperature. The result of the contact angle for each sample is an average value of 10 measurements of individual droplets. The Owens-Wendt method was used to calculate surface free energy.

## Results and Discussions

### FTIR spectroscopy

In order to examine the chemical structure of the obtained films, IR spectra were made. The spectra of the pure collagen film and samples with additives are presented in FIG. 1 and 2. The infrared spectra show the characteristic bands of collagen. The bands at approximately  $3300\text{ cm}^{-1}$  correspond to amide A [22]. Amide B appears at  $3060\text{--}3080\text{ cm}^{-1}$  and bands at about  $2930\text{ cm}^{-1}$  are related to the asymmetric stretching vibrations of  $-\text{CH}_2$  [22,23]. The intensity of the amide III band that occurs at about  $1230\text{ cm}^{-1}$  is related to the triple helical structure [24]. Wavenumbers for subsequent bands are shown in TABLE 1.

It was observed that amide I and amide II in each sample are at the same positions. The addition of GTA does not influence the band position of amide I and II, as well as of amide III for 1% collagen. The amide III band in the 2% collagen film is shifted to lower wavenumbers. For amide B, the addition of GTA results in a shift to higher wavenumbers for both collagen concentrations (1% and 2%). A shift of a band attributed to  $=\text{CH}_2$  stretching vibrations to lower wavenumbers is observed for 1% collagen films with the addition of the cross-linking agent, while for 2% films, there are no significant changes in this band. Small changes occur in amide A for 1% films with additives. The addition of GTA influences the intensity of bands (FIG. 1 and 2).

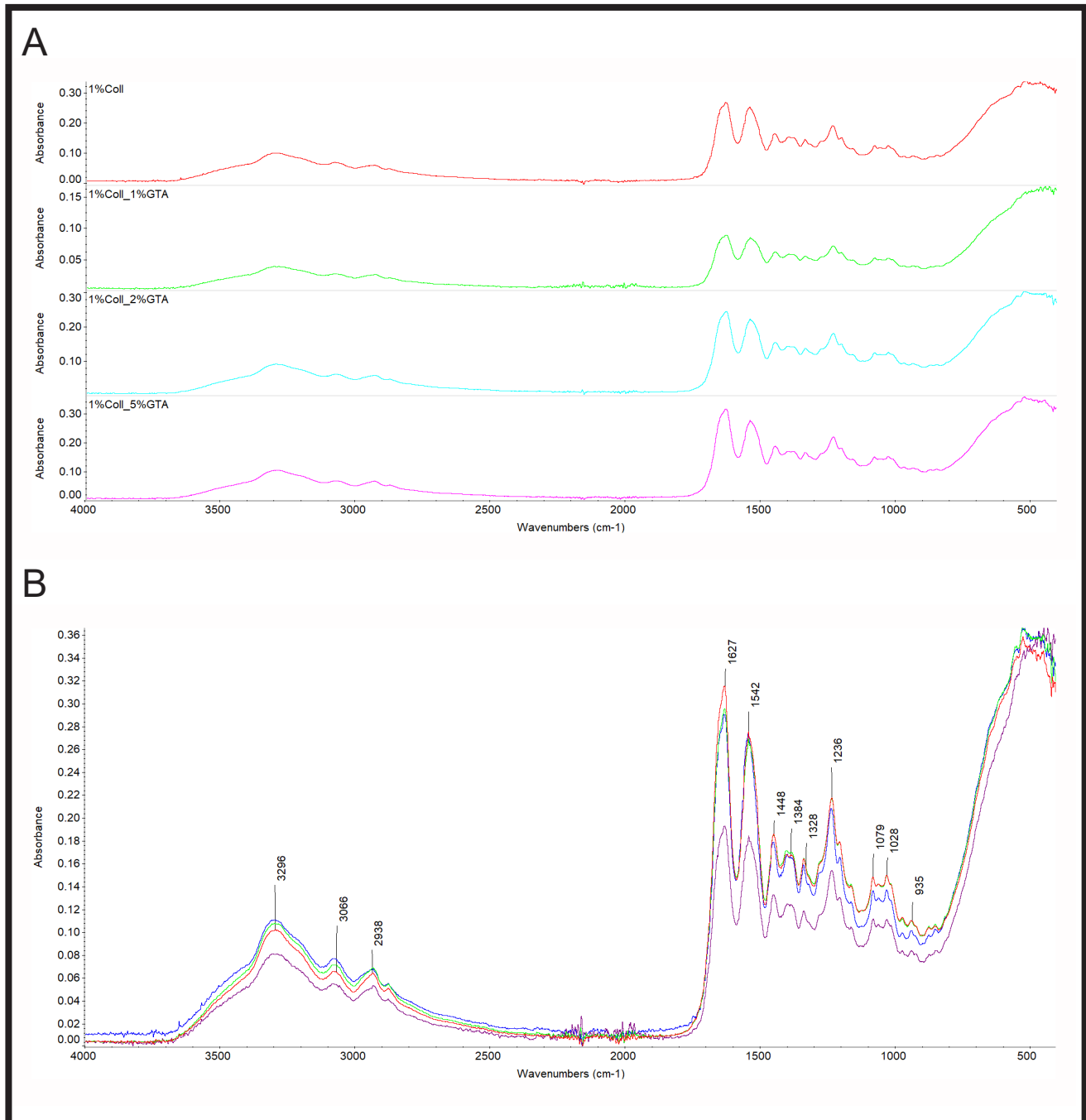


FIG. 1. The IR spectra of 1% collagen films cross-linked with GTA. Spectra are presented in stack (A) and overview (B). Wavenumber values are present for the main bands (B).

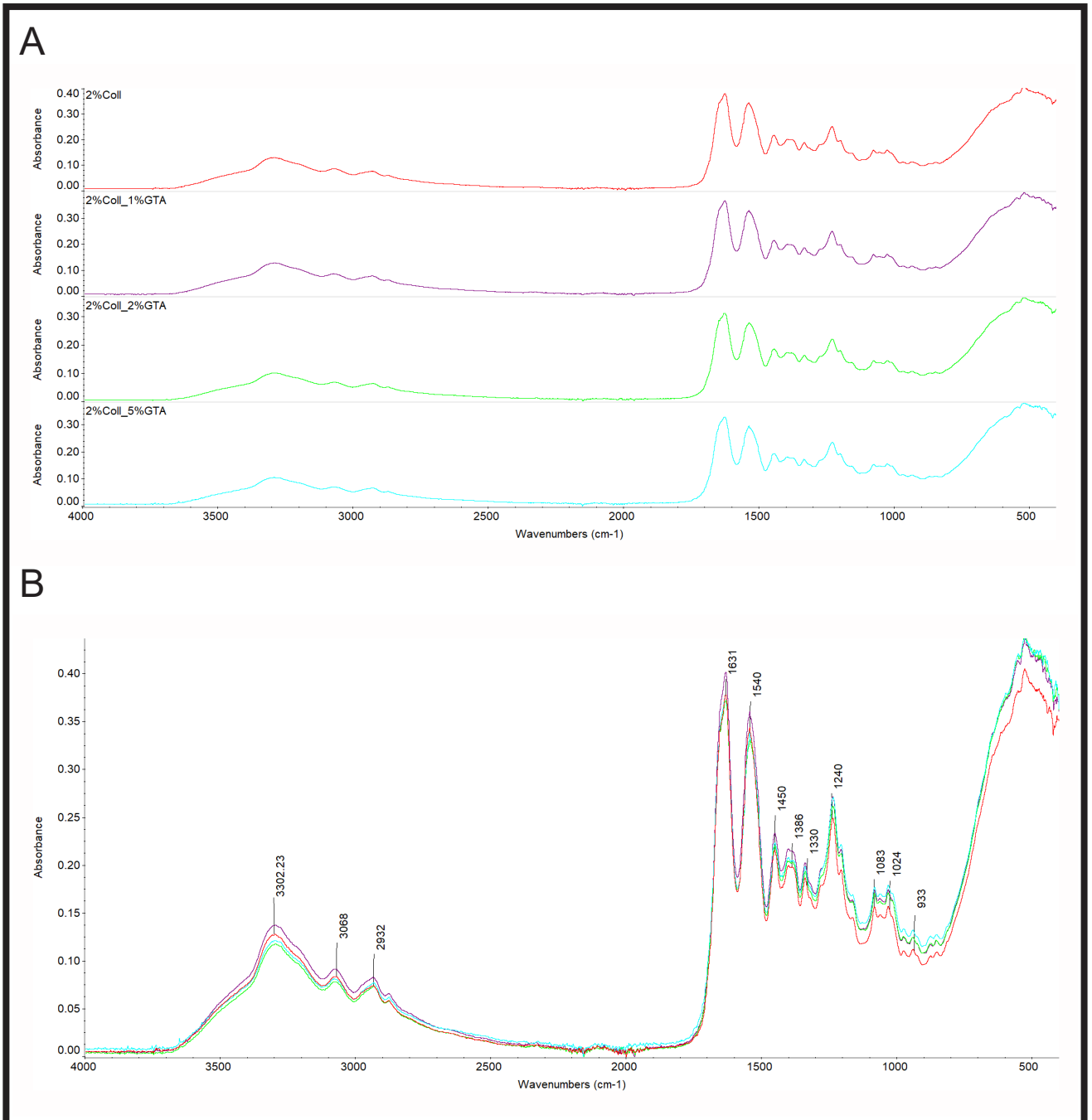


FIG. 2. The IR spectra of 2% collagen films cross-linked with GTA. Spectra are presented in stack (A) and overview (B). Wavenumber values are present for the main bands (B).

TABLE 1. Bands positions in IR spectra of collagen films with and without GTA.

Functional group vibrations		Amide A	Amide B	=CH <sub>2</sub>	Amide I	Amide II	Amide III
Wavenumber [cm <sup>-1</sup> ]	1%Coll	3296	3066	2938	1627	1542	1236
	1%Coll_1%GTA	3286	3076	2931	1630	1540	1232
	1%Coll_2%GTA	3294	3078	2931	1629	1541	1233
	1%Coll_5%GTA	3292	3077	2932	1631	1541	1233
	2%Coll	3302	3068	2932	1631	1540	1240
	2%Coll_1%GTA	3294	3077	2935	1629	1541	1234
	2%Coll_2%GTA	3293	3077	2930	1630	1540	1233
	2%Coll_5%GTA	3298	3076	2930	1632	1541	1232

**Mechanical properties**

The results of Young’s modulus, tensile strength, and elongation at break for thin collagen films without and with different concentrations of GTA are shown in FIG. 3. The concentration of collagen and addition of GTA affect the mechanical parameters of the samples.

Higher values of tensile strength, breaking force, and elongation at break were obtained for 2% collagen films in comparison to 1% films. Among all samples, the highest values of tensile strength, breaking force, and elongation at break were observed for samples with 1% of GTA, while the lowest for 5% GTA for 1% collagen. The latter was therefore the least flexible. One-way ANOVA was employed to examine differences in all mechanical properties between sample groups with different GTA concentrations.

**Contact angle**

The analysis indicated that all samples were hydrophilic. The addition of a cross-linking agent slightly decreased hydrophilicity. The values of the contact angle for glycerine were increased. The results are presented in TABLE 2 and FIG. 4.

**Swelling and degradation**

The swelling ratios of collagen films as a function of incubation time are presented in FIG. 5 and 6. The pure collagen films have fallen apart after 4 hours of incubation. The addition of the GTA increased the stability of samples up to 14 days, except for 2%Coll\_1%GTA. The swelling degrees of the 2% collagen films are significantly higher than the 1% films. In both cases, the highest values were obtained for samples cross-linked with 1% GTA. The increased amount of cross-linker is responsible for the lower swelling ability.

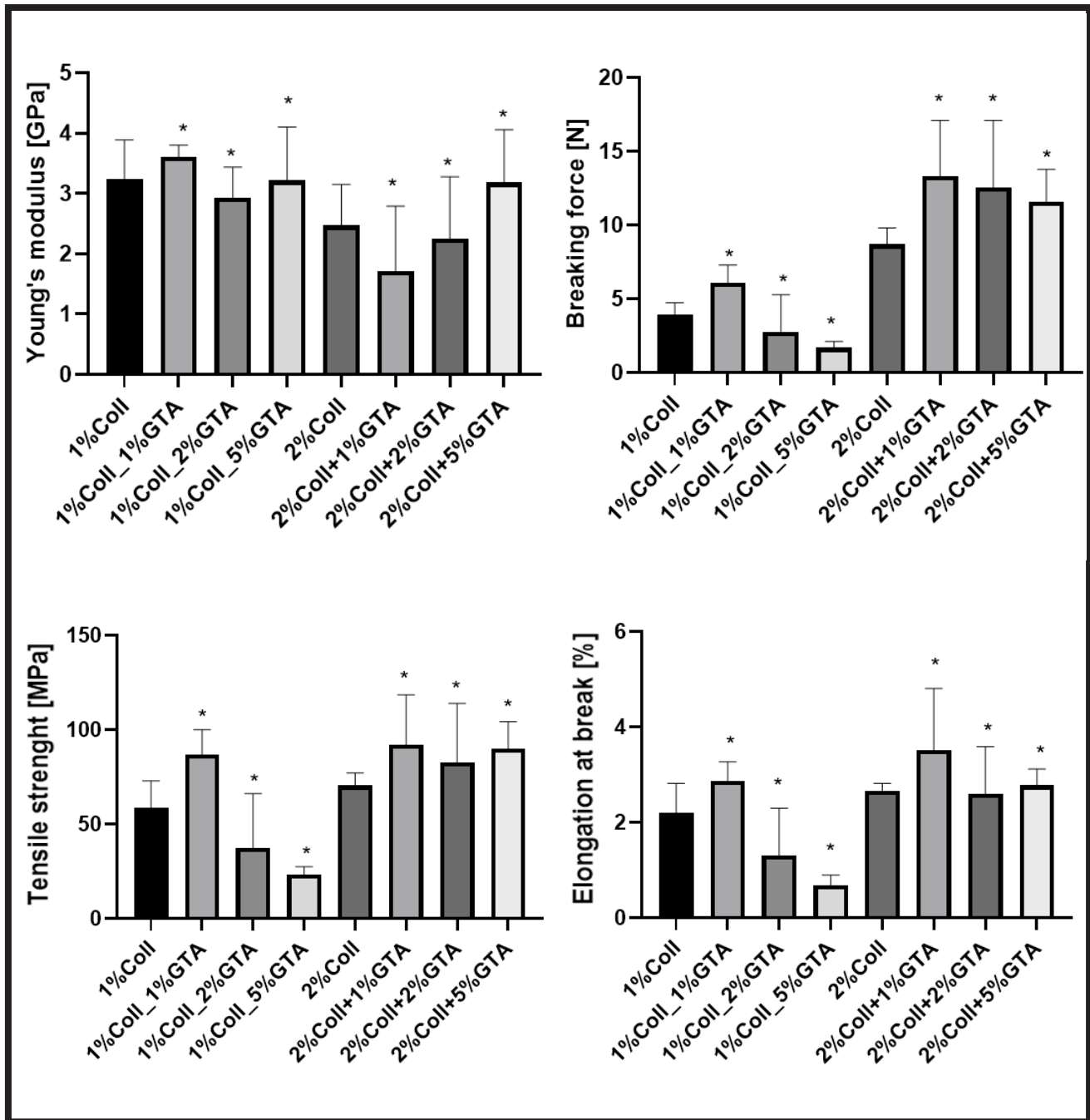


FIG. 3. Mechanical parameters of collagen films cross-linked with GTA; error bars represent standard deviation (SD) (significantly different from the respective control (p < 0.05) for all mechanical parameters).

TABLE 2. Contact angle results for collagen films not cross-linked and cross-linked with GTA.

Sample	$\Theta$ glycerine [°]	$\Theta$ diodomethane [°]	IFT (s) [mJ/m <sup>2</sup> ]	IFT (s, D) [mJ/m <sup>2</sup> ]	IFT (s, P) [mJ/m <sup>2</sup> ]
1%Coll	58.7	36.8	44.01	33.33	10.68
1%Coll_1%GTA	59.8	43.5	41.5	29.89	11.61
1%Coll_2%GTA	63.9	46	39.19	29.37	9.82
1%Coll_5%GTA	62.7	46	39.61	29.1	10.52
2%Coll	61.3	38.5	42.62	33.04	9.58
2%Coll_1%GTA	63.1	44.1	40.12	30.30	9.82
2%Coll_2%GTA	64.5	43.8	39.78	30.81	8.97
2%Coll_5%GTA	63	42.5	40.71	31.21	9.51

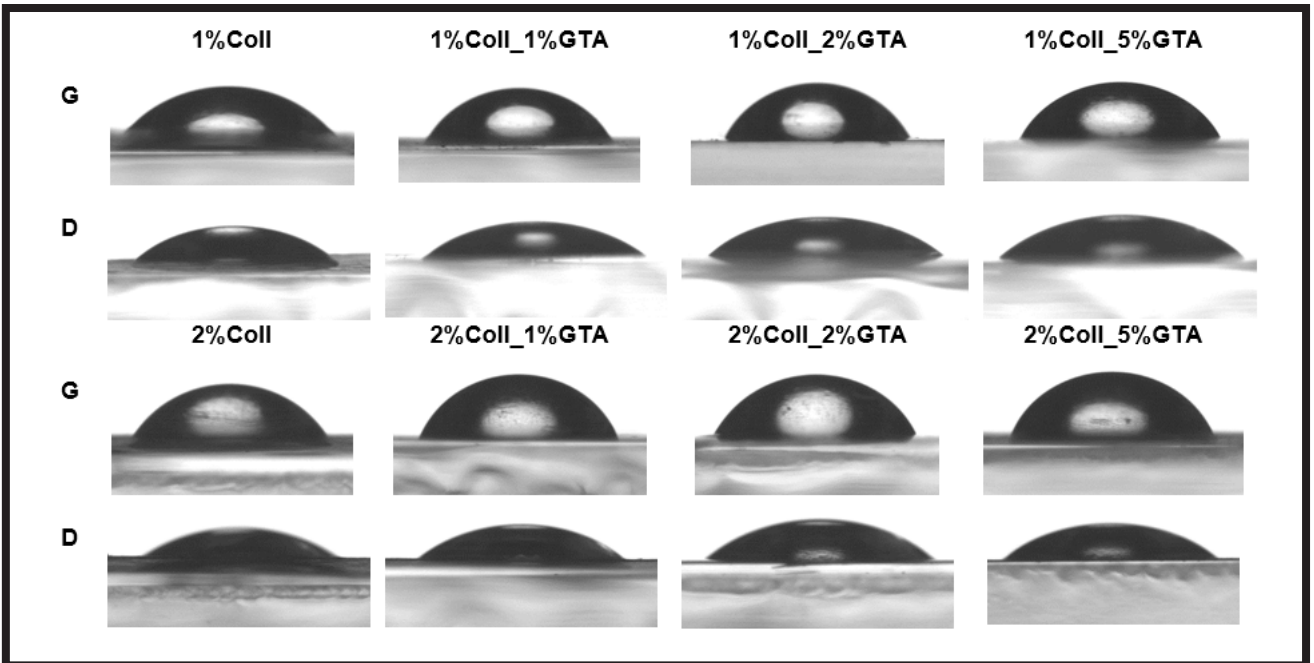


FIG. 4. Pictures of droplets during the contact angle measurement (G – glycerine, D – diodomethane).

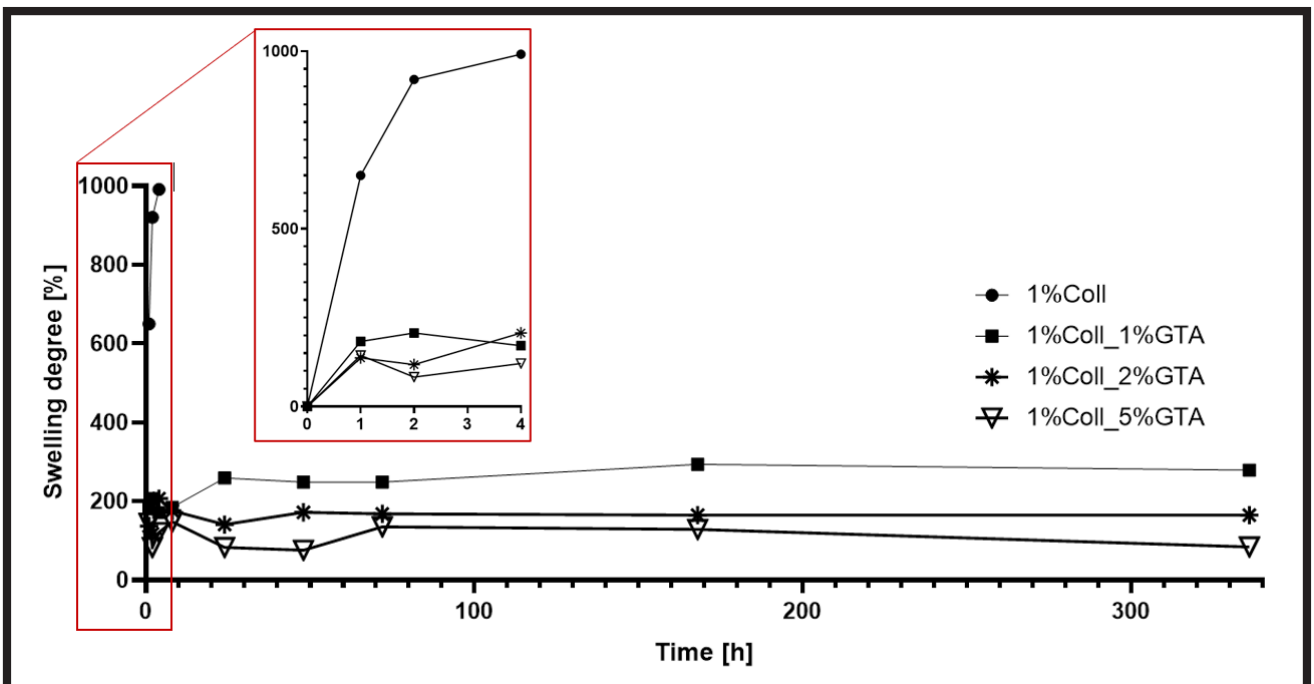


FIG. 5. Swelling degree of 1% collagen films non-cross-linked and cross-linked with GTA.

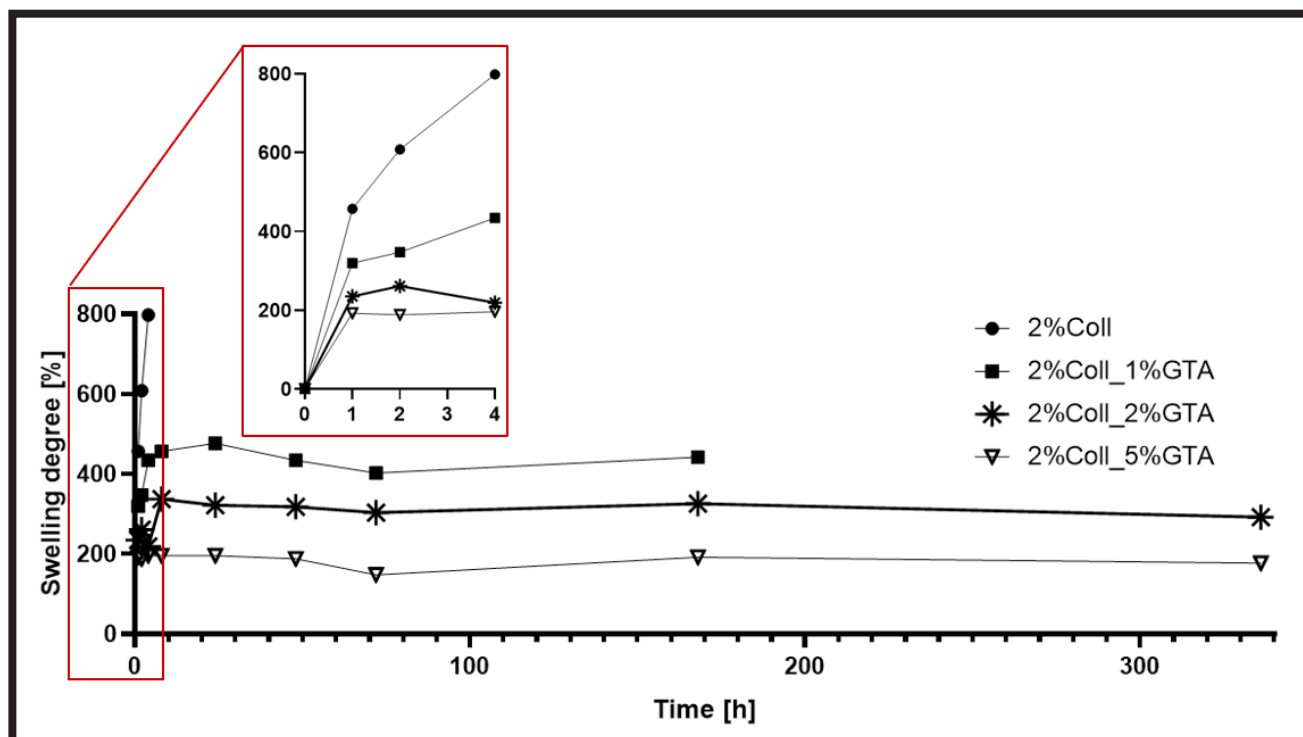


FIG. 6. Swelling degree of 2% collagen films non-cross-linked and cross-linked with GTA.

## Conclusions

The results of our research show that even small amounts of glutaraldehyde (GTA) added to the fish collagen change the properties of the films obtained. The IR analysis confirmed small changes in the chemical structure of all samples with GTA, which may be the result of the creation of hydrogen bonds. The addition of GTA causes changes in the intensity of the bands. The addition of GTA to collagen films influences the mechanical properties, swelling ability, and contact angle. 2% collagen films are characterized by lower Young's modulus values and are more susceptible to elongation compared to 1% collagen samples. 1%Coll+5%GTA was the least flexible between all samples studied. The amount of cross-linking agent added in relation to the amount of collagen is crucial for the final properties of the film. Samples containing 2% collagen have a greater amount of polymer with which GTA can interact. The swelling degrees were increased for 2% collagen samples compared to 1% collagen films, which is connected with the amount of biopolymer that can absorb more liquid. Samples modified with GTA were more stable than unmodified collagen films. Both pure collagen samples (1% and 2%) disintegrated after 4 h in PBS. The remaining samples were stable for up to 2 weeks. Swelling behaviour is an extremely important value in the design of active dressings; this is due to the function of wound dressings to collect exudate. Native collagen films had a lower contact angle for glycerine than GTA-modified samples. However, all of the samples were hydrophilic. Fish collagen films modified with GTA may be promising materials for applications in the biomedical field after testing their potential toxicity. In the case of glutaraldehyde, it is important to maintain a balance between the amount of reagent used and the expected results. An advantage of the proposed method is its simplicity and quickness.

## Acknowledgements

The authors acknowledge SanColl Company for preparing fish skin collagen for this research. The research was funded by NCBiR (grant number POIR.04.01.04-00-0077/20-00).

## ORCID iD

K. Kulka-Kamińska: <https://orcid.org/0000-0002-0825-1774>  
 P. Brudzyńska: <https://orcid.org/0000-0002-6646-1534>  
 A. Sionkowska: <https://orcid.org/0000-0002-1551-2725>  
 K. Lewandowska: <https://orcid.org/0000-0002-8380-4009>  
 Ł. Piwowarski: <https://orcid.org/0009-0000-6889-9209>

## References

- [1] Chen X., Zhou L., Xu H., Yamamoto M., Shinoda M., Kishimoto M., Tanaka T., Yamane H.: Effect of the Application of a Dehydrothermal Treatment on the Structure and the Mechanical Properties of Collagen Film. *Materials* 13 (2020) 377.
- [2] Bose S., Li S., Mele E., Williams C.J., Silberschmidt V.V.: Stability and mechanical performance of collagen films under different environmental conditions. *Polymer Degradation and Stability* 197 (2022) 109853.
- [3] Adamiak K., Sionkowska A.: Current methods of collagen cross-linking: Review. *International Journal of Biological Macromolecules* 161 (2020) 550-560.
- [4] Hwang S.J., Kim S.H., Seo W.-Y., Jeong Y., Shin M.C., Ryu D., Lee B. S., Choi Y.J., Kim K.: Effects of human collagen  $\alpha$ -1 type I-derived proteins on collagen synthesis and elastin production in human dermal fibroblasts. *BMB Reports* 54 (2021) 329-334.
- [5] Sionkowska A., Musiał K., Gadomska M., Adamiak K.: Fish collagen and chitosan mixtures as a promising biomaterial for potential use in biomedicine and cosmetic industry. *Engineering of Biomaterials* 164 (2022) 16-24.
- [6] Sionkowska A., Adamiak K., Musiał K., Gadomska M.: Collagen Based Materials in Cosmetic Applications: A Review. *Materials* 13 (2020) 4217.
- [7] Reilly D.M., Lozano J.: Skin collagen through the lifestages: importance for skin health and beauty. *Plastic and Aesthetic Research* 8 (2021) 2.
- [8] Darvish M.D.: Collagen fibril formation in vitro: From origin to opportunities. *Materials Today Bio* 15 (2022) 100322.
- [9] Davison-Kotler E., Marshall W.S., Garcia-Gareta E.: Sources of Collagen for Biomaterials in Skin Wound Healing. *Bioengineering* 6 (2019) 56.
- [10] Silvipriya K.S., Kumar K.K., Bhat A.R., Kumar D.B., John A., lakshamanan P.: Collagen: Animal Sources and Biomedical Application. *Journal of Applied Pharmaceutical Science* 5 (2015) 123-127.
- [11] Leon-Lopez A., Morales-Penaloza A., Martinez-Juarez V.M., Vargas-Torres A., Zeugolis D.I., Alvarez-Aguirre G.: Hydrolyzed Collagen – Sources and Applications. *Molecules* 24 (2019) 4031.
- [12] Nunez S.M., Guzman F., Valencia P., Almonacid S., Cardenas C.: Collagen as a source of bioactive peptides: A bioinformatics approach. *Electronic Journal of Biotechnology* 48 (2020) 101-108.
- [13] Felician F.F., Xia C., Qi W., Xu H.: Collagen from Marine Biological Sources and Medical Applications. *Chemistry & Biodiversity* 15(5) (2018) 1700557.
- [14] Blanco M., Vazquez J.A., Perez-Martin R.I., Sotelo C.G.: Hydrolysates of Fish Skin Collagen: An Opportunity for Valorizing Fish Industry Byproducts. *Marine Drugs* 15 (2017) 131.
- [15] Gallo N., Natali M.L., Quarta A., Gaballo A., Terzi A., Sibillano T., Giannini C., Benedetto G.E., Lunetti P., Capobianco L., Blasi F.S., Sicuro A., Corallo A., Sannino A., Salvatore L.: Aquaponics-Derived Tilapia Skin Collagen for Biomaterials Development. *Polymers* 14 (2022) 1865.
- [16] Dong Y., Dai Z.: Physicochemical, Structural and Antioxidant Properties of Collagens from the Swim Bladder of Four Fish Species. *Marine drugs* 20 (2022) 550.
- [17] Sionkowska A., Lewandowska K., Adamiak K.: The influence of uv light on rheological properties of collagen extracted from silver carp skin. *Materials* 13 (2020) 4453.
- [18] Islam M.M., AbuSamra D.B., Chivu A., Argueso P., Dohman C.H., Patra H.K., Chodosh J., Gonzales-Andrades M.: Optimization of Collagen Chemical Crosslinking to Restore Biocompatibility of Tissue-Engineering Scaffolds. *Pharmaceutics* 13 (2021) 832.
- [19] Nair M., Calahorra Y., Kar-Narayan S., Best S.M., Cameron R.E.: Self-assembly of collagen bundles and enhanced piezoelectricity induced by chemical crosslinking. *Nanoscale* 11 (2019) 15120.
- [20] Peng Y.Y., Glattauer V., Ramshaw J.A.M.: Stabilisation of Collagen Sponges by Glutaraldehyde Vapour Crosslinking. *International Journal of Biomaterials* 2017 (2017) 1-6.
- [21] Damink L.H.H.O., Dijkstra P.J., Luyn M.J.A., Wachem P.B., Nieuwenhuis P., Feijen J.: Glutaraldehyde as a crosslinking agent for collagen-based biomaterials. *Journal of Materials Science: Materials in Medicine* 6 (1995) 460-472.
- [22] Slimane E.B., Sadok S.: Collagen from Cartilaginous Fish By-Products for a Potential Application in Bioactive Film Composite. *Marine Drugs* 16 (2018) 211.
- [23] Sionkowska A., Wiśniewski M., Skopińska J., Mantovani D.: Effects of Solar Radiation on Collagen-Based Biomaterials. *International Journal of Photoenergy* 2006 (2006) 1-6.
- [24] Elango J., Bu Y., Bin B., Geevaretnam J., Robinson J.S., Wu W.: Effect of chemical and biological cross-linkers on mechanical and functional properties of shark catfish skin collagen films. *Food Bioscience* 17 (2017) 42-51.